bioRxiv preprint doi: https://doi.org/10.1101/270314; this version posted February 23, 2018. The copyright holder for this preprint (which was not certified by peer review) is the author/funder. All rights reserved. No reuse allowed without permission.

YAP1 Oncogene is a Context-specific Driver for Pancreatic Ductal Adenocarcinoma

Bo Tu[1#], Wantong Yao[2#], Jun Yao[1], Sammy Ferri-Borgogno[3,4], Shujuan Chen[1], Qiuyun Wang[1], Liang Yan[1], Cihui Zhu[1], Seungmin Bang[7], Qing Chang[5], Christopher A. Bristow[5], Yaan Kang[6], Hongwu Zheng[8], Huamin Wang[3], Jason B. Fleming[6], Michael Kim[6], Giulio F. Draetta[1,2,5], Duojia Pan[9], Anirban Maitra[3,4], Sonal Gupta[3,4*], Haoqiang Ying[1*]

[1]Departments of Molecular and Cellular Oncology, [2]Department of Genomic Medicine, [3]Department of Pathology, [4]Sheikh Ahmed Center for Pancreatic Cancer Research, [5]Institute for Applied Cancer Science, [6]Department of Surgical Oncology, University of Texas MD Anderson Cancer Center, Houston, Texas; [7]Department of Internal Medicine, Institute of Gastroenterology, Yonsei University College of Medicine, Seoul, Korea; [8]Cold Spring Harbor Laboratory, Cold Spring Harbor, New York; [9]Department of Physiology, Howard Hughes Medical Institute, University of Texas Southwestern Medical Center, Dallas, Texas.

 # These authors contributed equally to this work

***Corresponding Authors:** Sonal Gupta, PhD, Email: sgupta8@mdanderson.org.

Haoqiang Ying, MD, PhD, Email: hying@mdanderson.org.

Author Contributions: B.T., W.Y., S.F-B., S.C., Q.W., L.Y., and S.G. performed data collection and interpretation. J.Y., provided statistical and bioinformatics analysis. C.Z. and S.B. contributed to animal breeding. Q.C., C.B., Y.K., H.Z., H.W., J.F. and M.K. provided clinical specimen and data analyses on PDX samples. A.M. and H.W. performed pathology analyses. G.D., D.P. and A.M. provided crucial feedback on manuscript. S.G. and H.Y. drafted the manuscript. S.G. and H.Y. did conception, design and supervision of the study.

bioRxiv preprint doi: https://doi.org/10.1101/270314; this version posted February 23, 2018. The copyright holder for this preprint (which was not certified by peer review) is the author/funder. All rights reserved. No reuse allowed without permission.

Abstract

Objective: *Yap1* oncogene is essential for KRAS-induced pancreatic ductal adenocarcinoma (PDAC) initiation. We recently demonstrated that YAP1 is capable of bypassing KRAS-dependency. However, genetic alterations of YAP1 pathway are rare in human PDAC and its role in tumour maintenance remains unclear. This study investigates YAP1 function in transcriptionally distinct subsets of PDAC and explores the molecular mechanisms for YAP1 activation.

Design: Conditional *Yap1* allele was crossed into *LSL-Kras*$^{G12D/+}$; *Trp53*$^{R172H/+}$; *Mist1-Cre*$^{ERT2+}$ mice to study the requirement of *Yap1* for PDAC development in adult mice. YAP1 function in advanced PDAC was analyzed in human tissues, PDAC cell lines, patient-derived xenograft samples and mouse PDAC cells, using in vitro and in vivo assays and gene expression analyses. WNT5A expression and its effect on YAP1 activation as well as tumorigenic activity was studied in aforementioned human and mouse systems using genetic and pharmacological approaches. The bypass of KRAS-dependency by WNT5A was evaluated in *Kras*^{G12D}-driven mouse PDAC cells.

Results: *Yap1* deletion blocked *Kras*^{G12D}/*Trp53*$^{R172H/+}$ induced PDAC development in mice. YAP1 activation correlated with squamous subtype of human PDAC and poor prognosis. YAP1 activation enhanced malignant phenotype and YAP1 depletion suppressed the tumorigenic activity specifically in squamous subtype tumours. WNT5A was significantly overexpressed in squamous subtype tumours and positively correlated with YAP1 activity. Conversely, WNT5A depletion resulted in YAP1 inactivation and inhibition of tumorigenic activity. WNT5A expression enabled cell survival and tumour growth in the absence of oncogenic *Kras*.

Conclusions: YAP1 oncogene is a major driver for squamous subtype PDAC whose activation is mediated by WNT5A overexpression.

bioRxiv preprint doi: https://doi.org/10.1101/270314; this version posted February 23, 2018. The copyright holder for this preprint (which was not certified by peer review) is the author/funder. All rights reserved. No reuse allowed without permission.

Introduction

Pancreatic ductal adenocarcinoma, expected to become the second most common cause of cancer-related mortality in the US by 2030[1], is a highly heterogeneous disease with complex genetic and molecular diversity. While majority of PDACs share near-ubiquitous oncogenic mutations of *KRAS* and the frequent inactivation of *TP53*, *SMAD4* and *CDKN2A* tumour suppressors, most additional somatic mutations occur at low individual prevalence, suggesting diverse mechanisms underlying PDAC progression[2]. Although others and we have shown that *KRAS* oncogene is essential for tumour maintenance[3 4], effective targeting of KRAS pathway is yet to be achieved clinically. Moreover, recent studies have revealed a subpopulation of PDAC cells may bypass KRAS-dependency in advanced tumours[5-7], pointing to a critical need to identify context-specific vulnerabilities to improve patient outcome.

Recent large-scale molecular analyses have confirmed that human PDAC can be classified into several subtypes based on transcriptome profiles[8-11]. Although the subtype nomenclature varies between individual reports, the molecular signature of each subtype is largely overlapping across these studies. Since it has been suggested that the expression signatures of some of the subtypes, such as ADEX/exocrine or immunogenic subtype, are likely derived from non-neoplastic cells[9 11], the molecular signatures of tumour cells largely fall into two categories, namely the squamous/quasimesenchymal/basal-like and the progenitor/classical subtypes. Although the expression subtypes are not consistently associated with any somatic mutation or other genetically altered pathways[11], the squamous subtype reproducibly exhibits worse prognosis compared to other subtypes[8 10 11]. This suggest the biological phenotype of these tumour subgroups are driven by subtype-specific molecular mechanisms other than genetic alterations and thus, identifying the oncogenic pathways that

bioRxiv preprint doi: https://doi.org/10.1101/270314; this version posted February 23, 2018. The copyright holder for this preprint (which was not certified by peer review) is the author/funder. All rights reserved. No reuse allowed without permission.

drive the squamous subtype tumours will reveal subtype-specific vulnerabilities to treat these highly malignant tumours.

Yes-associated protein 1 (YAP1) is a transcriptional coactivator and plays critical roles in controlling tissue growth during organ development[12]. Its activity is kept in check by the upstream Hippo pathway, composed of the MST1/2-LATS1/2 kinases cascade, which phosphorylates YAP1 at multiple serine residues and sequesters YAP1 in cytoplasm for degradation[13]. Recent studies showed that YAP1 activation is commonly observed in tumour cells and in vivo studies using genetically engineered mouse (GEM) models have shown that hyper-activation of YAP1 results in acinar-to-ductal metaplasia, a trans-differentiation process tightly correlated with PDAC initiation[14 15]. Conversely, pancreas-specific *Yap1* deletion in GEM models abolished PDAC development driven by oncogenic *Kras*, suggesting YAP1 is essential for tumour initiation[16 17]. In addition, we recently showed that *Yap1* amplification is sufficient to bypass KRAS dependency in an inducible PDAC GEM model[5], implicating YAP1 may substitute oncogenic KRAS to sustain tumour growth. However, the requirement for YAP1 in tumour maintenance in advanced human PDAC is yet to be verified. Though, YAP1 is activated in human PDAC[16 18], the mechanisms that lead to YAP1 activation in PDAC cells remain largely elusive. Here we show that YAP1 is not only required for PDAC initiation in adult animals, but also remains activated in a subset of advanced human PDACs with squamous subtype feature and is required for their tumourigenic activity. We further identify WNT5A overexpression as one of the mechanisms leading to YAP1 activation in the deadliest form of PDAC.

Material and Methods

Transgenic Mice

For generation of tamoxifen-inducible PDAC GEM model, *Mist1*$^{Cre\text{ERT2/+}}$ [19] mice were used for conditional activation of mutant *Kras*^{G12D} and mutant *Trp53*^{R172H} in the mature pancreas. For *Yap1*

bioRxiv preprint doi: https://doi.org/10.1101/270314; this version posted February 23, 2018. The copyright holder for this preprint (which was not certified by peer review) is the author/funder. All rights reserved. No reuse allowed without permission.

deletion, these mice were further crossed with *Yap1*$^{fl/fl}$ mice[20]. For most efficient recombination, tamoxifen was administered (i.p.) to 6-week old mice in corn oil once daily for 5 days. The recombination efficiency was tested using PCR primers designed specifically to detect wildtype and recombinant alleles of *Kras*, *Trp53* and *Yap1* in pancreatic tissue. All manipulations were approved under MD Anderson Cancer Center (MDA) Institutional Animal Care and Use Committee (IACUC) under protocol number 00001549.

Xenograft Studies

All xenograft studies were carried out in NCr nude mice (Taconic) and were approved by the MD Anderson IACUC under protocol number 00001549. Details for the xenograft studies are described in Supplementary Methods.

Cell Culture and Establishment of Primary PDAC lines

Human pancreatic cell lines SNU410, HPAC, HPAFII, PL45, PaTu8988S and PaTu8988T were obtained from ATCC. Pa04C was established from resected patient tumours and maintained as low passage (<10)[21] and cultured according to recommended protocols. Establishment and maintenance of primary mouse PDAC lines was performed as described previously[4]. The human patient PDX cell lines were maintained in RPMI-1640 medium containing 10% FBS (Clontech).

Reagents

Doxycycline (RPI), PE Annexin V Apoptosis Detection Kit I (BD Biosciences), BOX5 (EMD Millipore).

Immunostaining and Western Blot Analysis

Immunohistochemical (IHC) analysis was performed as described earlier[22]. Details for immunofluorescence staining, western blot and primary antibody information are described in Supplementary Methods.

bioRxiv preprint doi: https://doi.org/10.1101/270314; this version posted February 23, 2018. The copyright holder for this preprint (which was not certified by peer review) is the author/funder. All rights reserved. No reuse allowed without permission.

Lentivirus Mediated shRNA Knockdown

All lentiviral shRNA clones targeting YAP1, WNT5A and non-targeting shRNA control were obtained from Sigma Aldrich in the pLKO vector. The clone IDs for the shRNA are listed in Supplementary Materials.

Crispr-Cas9 Mediated Gene Knockout (KO)

sgRNAs targeting mouse Wnt5a were cloned into pSpCas9(BB)-2A-Puro (Addgene, #62988) and transfected into target cells. After 2 μg/ml puromycin selection for 1 week, single cell clones are isolated and analyzed by T7E1 assay and Western blot. Sequences for *Wnt5a* sgRNA are listed in Supplementary Materials.

TMA staining and analysis

Immunohistochemical staining for YAP1 was performed on 5-μm unstained sections from the tissue microarray blocks, which included 92 (MD Anderson Cancer Center (MDA)) or 83 (Johns Hopkins University School of Medicine (JHU)) PDAC samples from patients who underwent upfront surgery. The immunohistochemical staining for YAP1 was reviewed by a pathologist (H.W.). The expression of YAP1 was classifies as YAP1-low and YAP1-high using the median score for total YAP1 expression (nuclear plus cytoplasmic expression) as a cutoff.

Statistical Analysis

Tumour volume and tumour free survivals were analyzed using GraphPad Prism. To assess distributional differences of variance across different test groups, the Mann-Whitney test was used. Other comparisons were performed using the unpaired Student t-test. For all experiments with error bars, standard deviation (SD) was calculated to indicate the variation with each experiments and data, and values represent mean ± SD.

Results

bioRxiv preprint doi: https://doi.org/10.1101/270314; this version posted February 23, 2018. The copyright holder for this preprint (which was not certified by peer review) is the author/funder. All rights reserved. No reuse allowed without permission.

YAP1 is required for PDAC development in adult mice

To evaluate the role of YAP1 in human PDAC, tissue microarray (TMA) analysis in a cohort of 92 human PDAC showed that 47% PDACs exhibit high YAP1 protein expression in tumour epithelium compared to surrounding stromal tissue. The median overall survival (OS) for YAP1-low group was 38.3 months compared to 25.3 months for YAP1-high group (p=0.02) (Fig.1A&B). Such association between elevated YAP1 protein and poor survival was further validated in an independent cohort of 83 PDAC patients (p=0.0475) (Fig.1C), implicating YAP1 may promote adverse biological outcomes in PDAC. The in vivo function of YAP1 during PDAC development was further characterized using genetically engineered mouse (GEM) models. Tamoxifen-induced acinar-specific activation of Cre recombinase in the *Mist1-Cre*^{ERT2}; *LSL-Kras*$^{G12D/+}$; *LSL-Trp53*$^{R172H/+}$ (MKP) model leads to rapid PDAC development accompanied by induction of nuclear YAP1 expression in tumour cells (Fig. 1D, *left*, YAP-WT). In contrast, acinar-specific deletion of *Yap1* in the MKPY (YAP-KO) model completely blocked tumour development, resulting in relatively normal pancreas (Fig.1D-F). While all MKP mice succumbed to PDAC with a median survival of 103 days (n=29), *Yap1*-null MKPY mice remained entirely free of any overt disease and pathological lesion (n=29) (Fig.1G). This could be attributed to the effect of YAP1 on cell proliferation and survival, as evident by loss of both Ki67 and survivin (BIRC5) staining in YAP-KO pancreas (Fig.1H & S1A). The protective effect of *Yap1* deletion on *Kras*^{G12D} and *Trp53*$^{R172H/+}$ -induced PDAC development was further confirmed with an independent tamoxifen-inducible *Elastase-Cre*^{ERT2}; *LSL-Kras*$^{G12D/+}$; *LSL-Trp53*$^{R172H/+}$ model (Fig.S1B).

YAP1 is activated in squamous subtype of human PDAC

Gain-of-function studies showed that ectopic expression of mutant YAP1^{S127A}, a constitutively active YAP1 resistant to cytoplasmic retention and degradation [13], drastically enhanced the anchorage-independent growth, migration and invasion capacity of human PDAC cell line PaTu8988S cells and

bioRxiv preprint doi: https://doi.org/10.1101/270314; this version posted February 23, 2018. The copyright holder for this preprint (which was not certified by peer review) is the author/funder. All rights reserved. No reuse allowed without permission.

Pa04C cells, an early passage patient-derived cell line (Fig.2A-C, S2A), suggesting active YAP1 may promote the tumorigenicity and metastatic spread of PDAC cells. Indeed, YAP1^{S127A} expression diminished necrotic regions within primary tumour core and greatly enhanced the distal metastasis of Pa04C cells in an orthotopic xenograft model (Fig.2D&E). This was accompanied by induction of canonical YAP1 target genes, such as *CYR61*, *CTGF* and *AXL* in both cultured cells and xenograft tumours (Fig.S2B&D), suggesting YAP1 activation contributing to this aggressive phenotype. Gene expression microarray and subsequent Gene Set Enrichment Analysis (GSEA) in these cells confirmed an established YAP1 signature (Fig.S2C), enrichment in pathways associated with tumour development and metastasis, and the underlying cellular processes responsible, such as cell proliferation, cell cycle progression, migration, motility and epithelial-to-mesenchymal transition (EMT) (Fig.S2E-G, Supplementary Tables 1-2). Upregulation of genes responsible for EMT were also confirmed by QPCR (Fig.S2H). Interestingly, cellular processes like cell cycle progression and signaling pathways significantly activated in Pa04C-YAP1^{S127A} such as MYC, IL6-STAT3, TGFβ, RhoA, E2F, TNF etc., along with Hippo signaling pathway were part of all four gene signatures (GP2-5) associated with squamous subtype of PDAC[8] (Supplementary Table 2-4), implicating the role of YAP1 activation in this most aggressive subtype.

To address this, we analyzed the expression profiles of human PDAC from the recent ICGC collection[8] and found significant enrichment of YAP1 activation signature[23] in tumours of squamous subtype (Fig.2F&G). YAP1 pathway activation is significantly correlated with poor survival in PDAC patients (Fig.2H). Squamous subtype has also been shown to be associated with poor prognosis[8 10]. Thus, to exclude the possibility that correlation between YAP1 activation and shortened patient survival is merely a reflection of enrichment of YAP1 signature in squamous subtype, we further analyzed the prognostic value of YAP1 signature in PDAC subtypes other than the squamous subtype. Indeed, the

bioRxiv preprint doi: https://doi.org/10.1101/270314; this version posted February 23, 2018. The copyright holder for this preprint (which was not certified by peer review) is the author/funder. All rights reserved. No reuse allowed without permission.

median patient survival significantly declines with the increase of YAP1 activation signature in those non-squamous subtype tumours (Fig.2I), indicating that YAP1 pathway activation is an independent prognosis factor in PDAC patients.

To further exclude the possibility that YAP1 activation signature in squamous subtype PDAC is largely derived from tumour stroma, we analyzed the transcriptome data of human PDAC cell lines from CCLE dataset and that of a collection of 47 PDAC PDX models, after the expression reads from murine host were omitted. We failed to identify cell lines or PDX models that are enriched with ADEX or immunogenic signatures (data not shown), consistent with the notion that the molecular signatures of these subtypes are likely derived from non-tumour cells[9]. Not surprisingly, the molecular signatures of human PDAC cell lines or PDXs mostly clustered under either progenitor or squamous subtype (Fig. S2I&J). In accordance with the analysis of ICGC data, YAP1 activation signature was consistently elevated in squamous subtype (Fig.2J&K). Interestingly, multiplexed gene expression analysis using the NanoString platform showed that, in contrast to the parental PaTu8988S cells that belonged to progenitor subtype, the molecular signature of PaTu8988S cells expressing YAP1^{S127A} was highly similar to that of PaTu8988T cells, which were derived from the same patient as PaTu8988S cells[24] but of squamous subtype (Fig.S2K), thus, indicating YAP1 activation is capable of driving the molecular signature of squamous subtype.

YAP1 is essential for the maintenance of squamous subtype PDACs

To further investigate the requirement of YAP1 in squamous subtype PDAC, we conducted loss-of-function studies with shRNA in a panel of human PDAC cell lines and early-passage primary cell lines derived from human PDX tumours. Knockdown of YAP1 strongly suppressed the colony formation capacity of PDAC cell lines (PaTu8988T, SNU410 and PL45) and PDX lines (PATC148 and PATC153) belonging to squamous subtype with strong YAP1 activation signature (Fig.3A-D). In

bioRxiv preprint doi: https://doi.org/10.1101/270314; this version posted February 23, 2018. The copyright holder for this preprint (which was not certified by peer review) is the author/funder. All rights reserved. No reuse allowed without permission.

contrast, progenitor subtype cell lines with low YAP1 signature, including PaTu8988S, HPAF-II, HPAC PATC102 and PATC108 cells, were less sensitive to YAP1 depletion (Fig.3A-D), indicating the critical role of YAP1 in squamous subtype PDAC.

Others and we have previously showed that YAP1 activation enables the bypass of oncogene addiction in multiple cancer types, including PDAC[5 25-27]. Indeed, compared to PaTu8988S cells, PaTu8988T cells were more resistant to KRAS knockdown with shRNA (Fig.3E-F&S3A). Expression of $YAP1^{S127A}$ partially rescued the growth of PaTu8988S cells upon KRAS depletion (Fig.3E-F&S3A), indicating that YAP1 activation could enable bypass of KRAS-dependence in PDAC cells. Accordingly, pathway analysis of human PDAC expression profiles in the ICGC dataset indicated that genes induced upon KRAS inhibition were significantly upregulated in squamous subtype tumours (Fig.S3B&C), implying relatively low KRAS activity in these tumours. By using an inducible $Kras^{G12D}$-driven PDAC GEM model, we have recently obtained a collection of spontaneous relapse tumours following $Kras^{G12D}$ extinction in advanced PDAC (iKras- tumours)[5]. These tumours neither expressed oncogenic *Kras* nor exhibited strong activation of KRAS surrogates, and are thus deemed as KRAS-independent. Interestingly, molecular signature of the iKras- tumours was also significantly enriched in squamous subtype of human PDACs (Fig.3G&S3D), further supporting the notion that squamous subtype tumours are relatively KRAS-independent. Consistent with the YAP1 activation in human squamous subtype PDAC, YAP1 signature is significantly enriched in the mouse iKras- tumours (Fig.3H). Moreover, while the growth of $Kras^{G12D}$-driven mouse PDAC cells was insensitive to YAP1 knockdown, YAP1 depletion largely blocked the colony formation capability of iKras- tumour cells (Fig.3I&J). Interestingly, re-induction of $KRAS^{G12D}$ expression with doxycycline in iKras- cells fails to sustain colony formation following YAP1 knockdown (Fig.S3E-G), suggesting YAP1 activation may render oncogenic KRAS obsolete in PDAC cells.

bioRxiv preprint doi: https://doi.org/10.1101/270314; this version posted February 23, 2018. The copyright holder for this preprint (which was not certified by peer review) is the author/funder. All rights reserved. No reuse allowed without permission.

YAP1 activation in PDAC is mediated by WNT5A overexpression

In an effort to identify mechanism for YAP1 activation, genomic analysis of primary human tumours from ICGC or TCGA dataset didn't reveal obvious copy number changes or mutations of *YAP1* locus (Fig.S4A). While *Yap1* is amplified in a subset of mouse iKras- tumours[5], most iKras- tumours harbor no genomic alteration of *Yap1* despite enrichment of YAP1 signature (Fig.S4B&3H), indicating non-genetic mechanisms cause YAP1 activation in PDAC. YAP1 activation occurs by its nuclear translocation [13], which indeed, was evident in YAP1-dependent human PDAC cells, including PaTu8988T, SNU410 and PL45 cells, and iKras- mouse tumours or the derived cell lines without *Yap1* amplification (*iKras- Yap1*$^{Amp-}$) (Fig.4A&B, S4C). Conversely, YAP1 was localized in both cytoplasm and nuclei in PDAC cells with weak YAP1 signature, such as PaTu8988S, HPAF-II and HPAC cells, as well as *Kras*^{G12D}-driven mouse tumours and iKras- tumours with *Yap1* amplification (*iKras- Yap1*$^{Amp+}$) (Fig.4A&B). Accordingly, YAP1 activated human and mouse PDAC cells exhibit reduced phosphorylation at S127, the target site for directly upstream LATS1/2 kinases, along with corresponding decrease in LATS1/2 phosphorylation, an indicator of LATS1/2 activity (Fig.S4D&E). Surprisingly, no obvious difference was observed for MST1/2 phosphorylation or their total protein level (Fig.S4E), suggesting YAP1 activation in PDAC cells was largely through direct modulation of LATS1/2 activity, independent of MST1/2.

To identify the mechanisms leading to YAP1 activation, we compared the differentially regulated pathways in *iKras- Yap1*$^{Amp-}$ vs *iKras- Yap1*$^{Amp+}$ cells with GSEA. Interestingly, one of the pathways significantly elevated in *iKras- Yap1*$^{Amp-}$ cells was non-canonical WNT pathway[28] (Fig.4C), which has been recently shown to suppresses Hippo signaling and activate YAP1 in adipocytes[29]. Importantly, a strong correlation between non-canonical WNT signature and YAP1 activation signature was observed in TCGA dataset (Fig.4D), suggesting control of YAP1 activation by non-canonical WNT

bioRxiv preprint doi: https://doi.org/10.1101/270314; this version posted February 23, 2018. The copyright holder for this preprint (which was not certified by peer review) is the author/funder. All rights reserved. No reuse allowed without permission.

pathway in PDAC. A survey of WNT ligands identified *Wnt5a*, the prototypic non-canonical WNT ligand[30], to be exclusively overexpressed in the *iKras- Yap1*$^{Amp-}$ tumour cells at both mRNA and protein levels (Fig.4F&S4F). Moreover, *WNT5A* expression was also significantly elevated in squamous subtype compared to progenitor subtype tumours in the TCGA dataset (Fig.4E). Deletion of *Wnt5a* with CRISPR in two independent *iKras- Yap1*$^{Amp-}$ tumour cell lines lead to the induction of YAP1 phosphorylation at S127, increase in cytoplasmic retention of YAP1 protein as well as downregulation of YAP1 downstream target genes (Fig.4G-I). Additionally, ectopic expression of *Wnt5a* in *Kras*^{G12D}-driven tumour cells lead to decrease in YAP1 phosphorylation (Fig.4J), further supporting the notion that WNT5A expression drives YAP1 activation in mouse PDAC cells. We further validated these findings in human PDAC cell lines where WNT5A expression was found to be highly elevated in the YAP1-dependent PaTu8988T cells, in contrast to PaTu8988S cells, derived from same patient but with low YAP1 activation (Fig.4F). Ectopic expression of WNT5A in PaTu8988S cells reduced YAP1 phosphorylation and enhanced YAP1 nuclear localization (Fig.4J&K). On the other hand, depletion of WNT5A in PaTu8988T cells with shRNA resulted in elevated YAP1 phosphorylation (Fig.4L). Taken together, our data strongly indicates that WNT5A overexpression leads to YAP1 activation in PDAC cells.

WNT5A overexpression enables tumour maintenance and bypass of KRAS-dependence

At functional level, *Wnt5a* deletion in *iKras- Yap1*$^{Amp-}$ tumour cells with CRISPR significantly inhibited colony formation (Fig.5A&B). In agreement with the genetic ablation, treatment with WNT5A antagonist, BOX-5, specifically abolished the colony formation ability of *iKras- Yap1*$^{Amp-}$ tumour cells, but not the *Yap1*$^{Amp+}$ cells (Fig.5C&D). Moreover, *Wnt5a* deletion also significantly inhibited xenograft tumour growth in vivo, which was rescued by reconstituted WNT5A expression (Fig.5E&F). Importantly, in contrast with the predominant nuclear staining of YAP1 in the parental *iKras- Yap1*$^{Amp-}$

bioRxiv preprint doi: https://doi.org/10.1101/270314; this version posted February 23, 2018. The copyright holder for this preprint (which was not certified by peer review) is the author/funder. All rights reserved. No reuse allowed without permission.

cells, *Wnt5a* knockout tumours exhibited significant amount of cytoplasmic YAP1, implicating the diminished tumour growth to decreased YAP1 activity (Fig.5G). Indeed, expression of constitutive active YAP1^{S127A} largely rescued the inhibitory effect of *Wnt5a* deletion on tumour growth (Fig.5F), thus indicating WNT5A overexpression in mouse PDAC cells promotes tumour growth by activating YAP1. In agreement with this notion, depletion of WNT5A in human PDAC cell line, PaTu8988T cells, significantly inhibited their colony formation ability (Fig.5I).

Since YAP1 activation can maintain tumour growth upon genetic extinction of KRAS oncogene in PDAC[5 27], we next investigated if WNT5A overexpression can also serve to bypass KRAS-dependency. Indeed, ectopic expression of WNT5A in KRAS-dependent PaTu8988S cells partially restored the colony formation upon KRAS depletion (Fig.6A). In addition, forced WNT5A expression in *Kras*^{G12D}-driven iKras tumour spheres was able to maintain cell viability upon extinction of *Kras*^{G12D} by doxycycline withdrawal whereas most control tumour cells expressing GFP underwent apoptosis (Fig.6B-D). Importantly, the survival effect of WNT5A upon *Kras*^{G12D} extinction was largely abolished upon YAP1 knockdown (Fig.6B-D), indicating that YAP1 is required for WNT5A-induced bypass of KRAS-dependence. Indeed, similar to the effect of YAP1^{S127A}, ectopic WNT5A expression in iKras tumour cells showed KRAS-independent tumour growth when injected orthotopically into nude mice, whereas GFP-expressing iKras tumour cells failed to induce tumour formation in the absence of doxycycline (Figure 6E-G). Notably, WNT5A-driven tumours showed lower MAPK activity and strong nuclear YAP1 accumulation as compared to *Kras*^{G12D}-driven tumours (Fig.6H). Together, these results indicate that WNT5A overexpression can activate YAP1 and substitute for oncogenic Kras-driven tumour maintenance.

WNT5A-YAP1 axis functions in primary human PDAC

bioRxiv preprint doi: https://doi.org/10.1101/270314; this version posted February 23, 2018. The copyright holder for this preprint (which was not certified by peer review) is the author/funder. All rights reserved. No reuse allowed without permission.

Since WNT5A is not frequently overexpressed in established human PDAC cell lines (data not shown), we further validated the WNT5A-YAP1 axis in our collection of PDAC PDXs. As shown in Fig.7A-C, *WNT5A* expression is highly elevated in squamous subtype tumours and is significantly correlated with YAP1 signature in both PDXs and TCGA dataset. Accordingly, WNT5A was highly expressed while YAP1 phosphorylation was relatively low in squamous subtype PATC148 and PATC153 cells, while two cell lines derived from progenitor subtype tumours, PATC102 and PATC108, exhibited elevated YAP1 phosphorylation along with absence of WNT5A expression (Fig.7D). This is in accordance with the elevated expression of YAP1 target gene CYR61 and the dependence on YAP1 oncogene in squamous subtype PDXs (Fig.3C-D, 7D).

Consistent with our findings in known human PDAC cell lines and primary mouse tumour lines, shRNA-mediated depletion of WNT5A in PDX-derived PATC148 ($Kras^{G12D}$) and PATC153 (*Kras* WT) cells caused increase in YAP1 phosphorylation, suppression of the colony formation ability and diminished tumour growth in vivo (Fig.7E-H), supporting the essential role of WNT5A for the tumorigenic activity. Consistent with the role of WNT5A in bypass of KRAS-dependence, knockdown of KRAS elicited less inhibition on the growth of high WNT5A expressing PATC148 ($KRAS^{G12D}$) cells compared to low WNT5A expressing PATC102 ($KRAS^{G12D}$) and PATC108 ($KRAS^{G12D}$) cells, with KRAS WT PATC153 cells being resistant to KRAS knockdown (Fig.7I&J). Together, our data indicates that WNT5A overexpression in squamous subtype PDACs is required for YAP1 activation and tumour growth.

Discussion

YAP1 is activated in many cancer types and has been shown to be essential for tumour initiation and progression, including pancreatic cancer[31]. In this study, we found that PDAC development driven by $Kras^{G12D}$ and $Trp53^{R172H}$ in adult mice was marked by YAP1 activation, evident by its strong nuclear expression in tumour epithelium (Fig.1D). Subsequently, concurrent deletion of *Yap1* in adult pancreas

bioRxiv preprint doi: https://doi.org/10.1101/270314; this version posted February 23, 2018. The copyright holder for this preprint (which was not certified by peer review) is the author/funder. All rights reserved. No reuse allowed without permission.

completely blocked PDAC development (Fig.1E-G). These results complement the previously reported studies where conditional *Yap1* deletion at early embryonic stage blocked mutant *KRAS*-driven initiation of acinar to ductal metaplasia (ADM), premalignant lesions and subsequent tumour formation in GEM models[16 17]. Immunohistochemical staining on these tumour tissues showed marked decrease in cell proliferation index, as measured by Ki-67 staining (Fig.S1A) and high Survivin (BIRC5) expression (Fig.1H). Since, Survivin expression overlapped with YAP1 expression in *Yap1*-WT PDAC but completely lost in *Yap1*-KO pancreas, it is likely regulated directly by YAP1 at transcription level, as shown in esophageal squamous cell carcinoma[32]. Survivin is a known anti-apoptotic protein, which is expressed only in tumour cells[33] and mostly during G2-mitotic phases of cell cycle[34]. The mostly nuclear expression of Survivin that is observed in YAP-WT tumour sections (Fig.1H) supports its predominant role in regulating cell cycle. Accordingly, higher Survivin expression was also in agreement with predominant gene signatures associated with cell cycle progression in Pa04C-YAP1^{S127A} cells (Table S2) and higher percentage of Pa04C-YAP1^{S127A} cells in G2/M phase by cell cycle analysis (data not shown).

We provided evidence that YAP1 is highly activated in squamous subtype PDACs and required for their tumorigenic function. Moreover, we show that enforced YAP1 activation was able to convert the gene expression signature of PDAC cells from progenitor to squamous subtype, further indicating that YAP1 may function as a major driver for squamous subtype tumours and thus could be a potential therapeutic target in this highly malignant subgroup. The squamous subtype PDAC was characterized by high expression of mesenchyme-associated genes with PDAC cell lines enriched within squamous subtype exhibiting features of EMT[8 10 35]. Moreover, the KRAS-independent mouse PDAC tumours, which were YAP1-dependent and reminiscent of squamous subtype tumours, were also highly enriched with EMT signature (data not shown), thus implicating YAP1 in promoting aggressive behavior of

bioRxiv preprint doi: https://doi.org/10.1101/270314; this version posted February 23, 2018. The copyright holder for this preprint (which was not certified by peer review) is the author/funder. All rights reserved. No reuse allowed without permission.

squamous subtype PDAC through EMT. In fact, YAP1 has been shown to be a potent inducer of EMT in tumour cells[27]. Recently, ZEB1, a key EMT transcription factor, was shown to be critical for PDAC metastasis[36], and required for the transcription of YAP1 downstream targets by direct bind with YAP1[37]. Further studies are warranted to verify whether EMT is indeed required for YAP1-driven aggressive behavior, such as metastasis in PDAC.

Despite the emerging role of *YAP1* as a major oncogene in multiple cancer types, genetic alterations of *YAP1* gene or its upstream Hippo pathway are relatively uncommon[38 39]. While *YAP1* amplification has been identified in hepatocellular carcinomas [40], it has not been reported in PDAC till date. Since, mutations in *NF2*, an upstream negative regulator of YAP1 activity, is only reported in around 1% of human PDAC[8], the activation of YAP1 in advanced human PDAC is likely due to non-genetic factors regulating inhibitory upstream Hippo kinases. Our data showing constitutive nuclear localization of YAP1 protein in YAP1-dependent tumour cells, indicates that the suppression of Hippo signaling is the major mechanism for YAP1 activation in PDAC. While investigating upstream regulator of YAP1 activation, we found evidence that WNT5A overexpression leads to YAP1 activation and bypass of KRAS-dependency in KRAS-independent mouse PDAC cells and a subset of human squamous subtype PDACs. WNT5A is a prototypic non-canonical WNT ligand[30] and has been implicated in the pathogenesis of PDAC[41 42]. It has been recently shown that WNT5A-mediated non-canonical WNT pathway suppresses Hippo signaling and activates YAP1 through G protein-dependent activation of Rho GTPases[29]. WNT5A can also engage multiple additional downstream signaling pathways, including SRC and PKC, which have been shown to activate YAP1 through direct phosphorylation or indirectly through the regulation of Rho GTPases and LATS activity[43-48]. Interestingly, it was recently reported that non-canonical WNT and FZD8 mediated calcium signaling counteracts the tumourigenic activity of oncogenic KRAS[49]. On the other hand, FZD1 was shown to be

bioRxiv preprint doi: https://doi.org/10.1101/270314; this version posted February 23, 2018. The copyright holder for this preprint (which was not certified by peer review) is the author/funder. All rights reserved. No reuse allowed without permission.

important for WNT5A-mediated YAP1 activation[29]. It's possible that the engagement of specific receptors by WNT5A determines its signaling and biological output in PDAC. It remains to be further validated if any particular one or all of these mechanisms are responsible for WNT5A-mediated YAP1 activation in PDAC.

While our data indicates WNT5A overexpression in tumour cells functions in cell-autonomous manner to activate YAP1 oncoprotein, tumour cells may also get active WNT5A signaling through paracrine mechanisms. Indeed, WNT5A has been shown to be highly expressed in PDAC stroma fibroblast[50 51], and thus, stromal WNT5A could possibly contributes to YAP1 activation in tumour cells, given that the exuberant desmoplastic stroma is a defining characteristic of PDAC[2]. In this scenario, the tumour-stroma interaction will thus play an instrumental role in orchestrating the heterogeneous YAP1 activation in bulk tumour which may, in turn, define the molecular heterogeneity and diverse biological phenotypes of PDAC.

Taken together, with agents targeting the Hippo-YAP pathway under development[38], our study showing the critical role of WNT5A-mediated YAP1 activation in a subset of pancreatic tumours of squamous subtype provides viable therapeutic targets for this most malignant form of human PDAC.

Acknowledgements

We would like to thank the Institute for Applied Cancer Science (IACS), the Flow Cytometry and Cellular Imaging Core, the Department of Veterinary Medicine at The University of Texas MD Anderson Cancer Center (Cancer Center Support Grant, CA016672). We thank Dr. Ronald DePinho, Dr. Alan Wang, Dr. Mien-Chie Hung, Dr. Guocan Wang, Dr. Baoli Hu, Dr. Xin Zhou and Dr. Jihye Paik for helpful discussions and critical reviews. The research was supported by Hirshberg foundation for pancreatic cancer research and the Pancreatic Cancer Action Network-AACR Career Development

bioRxiv preprint doi: https://doi.org/10.1101/270314; this version posted February 23, 2018. The copyright holder for this preprint (which was not certified by peer review) is the author/funder. All rights reserved. No reuse allowed without permission.

Award to H.Y.; the Pancreatic Cancer Action Network-AACR Pathway to Leadership Award to W.Y.; P01 Grant (P01CA117969 12, NIH) to H.W., J.B.F., M.K., G.F.D., A.M. and H.Y.

bioRxiv preprint doi: https://doi.org/10.1101/270314; this version posted February 23, 2018. The copyright holder for this preprint (which was not certified by peer review) is the author/funder. All rights reserved. No reuse allowed without permission.

Reference:

1. Rahib L, Smith BD, Aizenberg R, et al. Projecting cancer incidence and deaths to 2030: the unexpected burden of thyroid, liver, and pancreas cancers in the United States. *Cancer Res* 2014;74(11):2913-21. doi: 10.1158/0008-5472.CAN-14-0155
2. Ying H, Dey P, Yao W, et al. Genetics and biology of pancreatic ductal adenocarcinoma. *Genes Dev* 2016;30(4):355-85. doi: 10.1101/gad.275776.115
3. Collins MA, Bednar F, Zhang Y, et al. Oncogenic Kras is required for both the initiation and maintenance of pancreatic cancer in mice. *J Clin Invest* 2012;122(2):639-53. doi: 10.1172/JCI59227 [published Online First: 2012/01/11]
4. Ying H, Kimmelman AC, Lyssiotis CA, et al. Oncogenic Kras maintains pancreatic tumors through regulation of anabolic glucose metabolism. *Cell* 2012;149(3):656-70. doi: 10.1016/j.cell.2012.01.058 [published Online First: 2012/05/01]
5. Kapoor A, Yao W, Ying H, et al. Yap1 activation enables bypass of oncogenic Kras addiction in pancreatic cancer. *Cell* 2014;158(1):185-97. doi: 10.1016/j.cell.2014.06.003 [published Online First: 2014/06/24]
6. Muzumdar MD, Chen PY, Dorans KJ, et al. Survival of pancreatic cancer cells lacking KRAS function. *Nat Commun* 2017;8(1):1090. doi: 10.1038/s41467-017-00942-5
7. Viale A, Pettazzoni P, Lyssiotis CA, et al. Oncogene ablation-resistant pancreatic cancer cells depend on mitochondrial function. *Nature* 2014;514(7524):628-32. doi: 10.1038/nature13611 [published Online First: 2014/08/15]
8. Bailey P, Chang DK, Nones K, et al. Genomic analyses identify molecular subtypes of pancreatic cancer. *Nature* 2016;531(7592):47-52. doi: 10.1038/nature16965
9. Cancer Genome Atlas Research Network. Electronic address aadhe, Cancer Genome Atlas Research N. Integrated Genomic Characterization of Pancreatic Ductal Adenocarcinoma. *Cancer Cell* 2017;32(2):185-203 e13. doi: 10.1016/j.ccell.2017.07.007
10. Collisson EA, Sadanandam A, Olson P, et al. Subtypes of pancreatic ductal adenocarcinoma and their differing responses to therapy. *Nat Med* 2011;17(4):500-3. doi: 10.1038/nm.2344 [published Online First: 2011/04/05]
11. Moffitt RA, Marayati R, Flate EL, et al. Virtual microdissection identifies distinct tumor- and stroma-specific subtypes of pancreatic ductal adenocarcinoma. *Nat Genet* 2015;47(10):1168-78. doi: 10.1038/ng.3398
12. Meng Z, Moroishi T, Guan KL. Mechanisms of Hippo pathway regulation. *Genes Dev* 2016;30(1):1-17. doi: 10.1101/gad.274027.115
13. Zhao B, Wei X, Li W, et al. Inactivation of YAP oncoprotein by the Hippo pathway is involved in cell contact inhibition and tissue growth control. *Genes Dev* 2007;21(21):2747-61. doi: 10.1101/gad.1602907 [published Online First: 2007/11/03]
14. Gao T, Zhou D, Yang C, et al. Hippo signaling regulates differentiation and maintenance in the exocrine pancreas. *Gastroenterology* 2013;144(7):1543-53, 53 e1. doi: 10.1053/j.gastro.2013.02.037 [published Online First: 2013/03/05]
15. Kopp JL, von Figura G, Mayes E, et al. Identification of Sox9-dependent acinar-to-ductal reprogramming as the principal mechanism for initiation of pancreatic ductal adenocarcinoma. *Cancer Cell* 2012;22(6):737-50. doi: 10.1016/j.ccr.2012.10.025
16. Gruber R, Panayiotou R, Nye E, et al. YAP1 and TAZ Control Pancreatic Cancer Initiation in Mice by Direct Upregulation of JAK-STAT3 Signaling. *Gastroenterology* 2016 doi: 10.1053/j.gastro.2016.05.006

bioRxiv preprint doi: https://doi.org/10.1101/270314; this version posted February 23, 2018. The copyright holder for this preprint (which was not certified by peer review) is the author/funder. All rights reserved. No reuse allowed without permission.

17. Zhang W, Nandakumar N, Shi Y, et al. Downstream of mutant KRAS, the transcription regulator YAP is essential for neoplastic progression to pancreatic ductal adenocarcinoma. *Sci Signal* 2014;7(324):ra42. doi: 10.1126/scisignal.2005049
18. Morvaridi S, Dhall D, Greene MI, et al. Role of YAP and TAZ in pancreatic ductal adenocarcinoma and in stellate cells associated with cancer and chronic pancreatitis. *Sci Rep* 2015;5:16759. doi: 10.1038/srep16759
19. Habbe N, Shi G, Meguid RA, et al. Spontaneous induction of murine pancreatic intraepithelial neoplasia (mPanIN) by acinar cell targeting of oncogenic Kras in adult mice. *Proc Natl Acad Sci U S A* 2008;105(48):18913-8. doi: 10.1073/pnas.0810097105
20. Cai J, Zhang N, Zheng Y, et al. The Hippo signaling pathway restricts the oncogenic potential of an intestinal regeneration program. *Genes Dev* 2010;24(21):2383-8. doi: 10.1101/gad.1978810
21. Jones S, Zhang X, Parsons DW, et al. Core signaling pathways in human pancreatic cancers revealed by global genomic analyses. *Science* 2008;321(5897):1801-6. doi: 10.1126/science.1164368 [published Online First: 2008/09/06]
22. Aguirre AJ, Bardeesy N, Sinha M, et al. Activated Kras and Ink4a/Arf deficiency cooperate to produce metastatic pancreatic ductal adenocarcinoma. *Genes Dev* 2003;17(24):3112-26.
23. Cordenonsi M, Zanconato F, Azzolin L, et al. The Hippo transducer TAZ confers cancer stem cell-related traits on breast cancer cells. *Cell* 2011;147(4):759-72. doi: 10.1016/j.cell.2011.09.048
24. Elsasser HP, Lehr U, Agricola B, et al. Establishment and characterisation of two cell lines with different grade of differentiation derived from one primary human pancreatic adenocarcinoma. *Virchows Arch B Cell Pathol Incl Mol Pathol* 1992;61(5):295-306.
25. Kim MH, Kim J, Hong H, et al. Actin remodeling confers BRAF inhibitor resistance to melanoma cells through YAP/TAZ activation. *EMBO J* 2016;35(5):462-78. doi: 10.15252/embj.201592081
26. Lin L, Sabnis AJ, Chan E, et al. The Hippo effector YAP promotes resistance to RAF- and MEK-targeted cancer therapies. *Nat Genet* 2015;47(3):250-6. doi: 10.1038/ng.3218
27. Shao DD, Xue W, Krall EB, et al. KRAS and YAP1 converge to regulate EMT and tumor survival. *Cell* 2014;158(1):171-84. doi: 10.1016/j.cell.2014.06.004
28. Schaefer CF, Anthony K, Krupa S, et al. PID: the Pathway Interaction Database. *Nucleic Acids Res* 2009;37(Database issue):D674-9. doi: 10.1093/nar/gkn653
29. Park HW, Kim YC, Yu B, et al. Alternative Wnt Signaling Activates YAP/TAZ. *Cell* 2015;162(4):780-94. doi: 10.1016/j.cell.2015.07.013
30. van Amerongen R. Alternative Wnt pathways and receptors. *Cold Spring Harb Perspect Biol* 2012;4(10) doi: 10.1101/cshperspect.a007914
31. Zanconato F, Cordenonsi M, Piccolo S. YAP/TAZ at the Roots of Cancer. *Cancer Cell* 2016;29(6):783-803. doi: 10.1016/j.ccell.2016.05.005
32. Muramatsu T, Imoto I, Matsui T, et al. YAP is a candidate oncogene for esophageal squamous cell carcinoma. *Carcinogenesis* 2011;32(3):389-98. doi: 10.1093/carcin/bgq254
33. Ambrosini G, Adida C, Altieri DC. A novel anti-apoptosis gene, survivin, expressed in cancer and lymphoma. *Nature medicine* 1997;3(8):917-21.
34. Caldas H, Jiang Y, Holloway MP, et al. Survivin splice variants regulate the balance between proliferation and cell death. *Oncogene* 2005;24(12):1994-2007. doi: 10.1038/sj.onc.1208350
35. Singh A, Settleman J. Oncogenic K-ras "addiction" and synthetic lethality. *Cell Cycle* 2009;8(17):2676-7. doi: 9336 [pii] [published Online First: 2009/08/20]
36. Krebs AM, Mitschke J, Lasierra Losada M, et al. The EMT-activator Zeb1 is a key factor for cell plasticity and promotes metastasis in pancreatic cancer. *Nat Cell Biol* 2017;19(5):518-29. doi: 10.1038/ncb3513

bioRxiv preprint doi: https://doi.org/10.1101/270314; this version posted February 23, 2018. The copyright holder for this preprint (which was not certified by peer review) is the author/funder. All rights reserved. No reuse allowed without permission.

37. Lehmann W, Mossmann D, Kleemann J, et al. ZEB1 turns into a transcriptional activator by interacting with YAP1 in aggressive cancer types. *Nat Commun* 2016;7:10498. doi: 10.1038/ncomms10498
38. Harvey KF, Zhang X, Thomas DM. The Hippo pathway and human cancer. *Nat Rev Cancer* 2013;13(4):246-57. doi: 10.1038/nrc3458 [published Online First: 2013/03/08]
39. Yu FX, Zhao B, Guan KL. Hippo Pathway in Organ Size Control, Tissue Homeostasis, and Cancer. *Cell* 2015;163(4):811-28. doi: 10.1016/j.cell.2015.10.044
40. Zender L, Spector MS, Xue W, et al. Identification and validation of oncogenes in liver cancer using an integrative oncogenomic approach. *Cell* 2006;125(7):1253-67. doi: 10.1016/j.cell.2006.05.030 [published Online First: 2006/07/04]
41. Schwartz AL, Malgor R, Dickerson E, et al. Phenylmethimazole decreases Toll-like receptor 3 and noncanonical Wnt5a expression in pancreatic cancer and melanoma together with tumor cell growth and migration. *Clin Cancer Res* 2009;15(12):4114-22. doi: 10.1158/1078-0432.CCR-09-0005
42. Ripka S, Konig A, Buchholz M, et al. WNT5A--target of CUTL1 and potent modulator of tumor cell migration and invasion in pancreatic cancer. *Carcinogenesis* 2007;28(6):1178-87. doi: 10.1093/carcin/bgl255
43. Gong R, Hong AW, Plouffe SW, et al. Opposing roles of conventional and novel PKC isoforms in Hippo-YAP pathway regulation. *Cell Res* 2015;25(8):985-8. doi: 10.1038/cr.2015.88
44. Grzeschik NA, Parsons LM, Allott ML, et al. Lgl, aPKC, and Crumbs regulate the Salvador/Warts/Hippo pathway through two distinct mechanisms. *Current biology : CB* 2010;20(7):573-81. doi: 10.1016/j.cub.2010.01.055
45. Kim NG, Gumbiner BM. Adhesion to fibronectin regulates Hippo signaling via the FAK-Src-PI3K pathway. *J Cell Biol* 2015;210(3):503-15. doi: 10.1083/jcb.201501025
46. Li P, Silvis MR, Honaker Y, et al. alphaE-catenin inhibits a Src-YAP1 oncogenic module that couples tyrosine kinases and the effector of Hippo signaling pathway. *Genes Dev* 2016;30(7):798-811. doi: 10.1101/gad.274951.115
47. Sudol M. Yes-associated protein (YAP65) is a proline-rich phosphoprotein that binds to the SH3 domain of the Yes proto-oncogene product. *Oncogene* 1994;9(8):2145-52.
48. Zaidi SK, Sullivan AJ, Medina R, et al. Tyrosine phosphorylation controls Runx2-mediated subnuclear targeting of YAP to repress transcription. *EMBO J* 2004;23(4):790-9. doi: 10.1038/sj.emboj.7600073
49. Wang MT, Holderfield M, Galeas J, et al. K-Ras Promotes Tumorigenicity through Suppression of Non-canonical Wnt Signaling. *Cell* 2015;163(5):1237-51. doi: 10.1016/j.cell.2015.10.041
50. Pilarsky C, Ammerpohl O, Sipos B, et al. Activation of Wnt signalling in stroma from pancreatic cancer identified by gene expression profiling. *J Cell Mol Med* 2008;12(6B):2823-35. doi: 10.1111/j.1582-4934.2008.00289.x
51. Seino T, Kawasaki S, Shimokawa M, et al. Human Pancreatic Tumor Organoids Reveal Loss of Stem Cell Niche Factor Dependence during Disease Progression. *Cell Stem Cell* 2018 doi: 10.1016/j.stem.2017.12.009

bioRxiv preprint doi: https://doi.org/10.1101/270314; this version posted February 23, 2018. The copyright holder for this preprint (which was not certified by peer review) is the author/funder. All rights reserved. No reuse allowed without permission.

Figure Legends

Figure 1. YAP1 is essential for PDAC development.

(A) Representative images of YAP1 TMA showing samples with low/no YAP1 level. (B-C) Kaplan-Meier curves for overall survival in PDAC patients from MDA (B) or JHU (C) stratified by YAP1 expression. (D) *Yap1* wild-type (WT) or knockout (KO) MKP mice driven by tamoxifen-inducible *Mist1-Cre*^{ERT2}. Pancreata were collected at indicated time points and YAP1 staining shows YAP1 activation in PDAC tumours of MKP mice. Gross images of pancreata (E) and H&E staining (F) shows block of tumour development in *Yap1*-KO mice. (G) Kaplan-Meier overall survival analysis for mice of indicated genotypes shows complete survival of *Yap1*-KO mice in contrast with median survival of 103 days in *Yap1*-WT mice. (H) Pancreata from *Yap1* wild-type (WT) or knockout (KO) MKP mice were collected at indicated time points and stained for Survivin. p value for survival analysis was calculated with log rank test.

Figure 2. YAP1 enhances the malignant phenotypes of PDAC and is activated in squamous subtype.

(A) Ectopic expression of YAP1^{S127A} in PaTu8988S and Pa04C cells promotes anchorage-independent growth in soft agar (quantification from triplicates shown in bottom panel) and cell invasion in a Boyden chamber assay (B) (Quantification of triplicates is shown in (C)). (D) Orthotopic xenograft tumours from Pa04C-Vector or -YAP1^{S127A} cells were established in immunocompromised mice (top). Red arrows indicate primary tumours and white arrows indicate metastatic tumours grown on peritoneum, lymph node and liver. Metastasis rate and involved organs are summarized in bottom panel. (E) H&E staining of orthotopic primary and metastatic tumours generated from Pa04C cells shows large necrotic areas in Pa04C-Vector tumours only while confirming metastases of Pa04C-YAP1^{S127A} (mYAP) cells in liver (Liv), lung (Lu), diaphragm (Dia) and lymph node (LN). (F) YAP1 signature score among human

bioRxiv preprint doi: https://doi.org/10.1101/270314; this version posted February 23, 2018. The copyright holder for this preprint (which was not certified by peer review) is the author/funder. All rights reserved. No reuse allowed without permission.

PDAC subtypes. Heatmap of the YAP1 signature gene expression is shown in (G). ADEX (A): aberrantly differentiated endocrine exocrine subtype; Immu (I): immunogenic subtype; Pro (P): progenitor subtype; SQ (S): squamous subtype. (H) Kaplan-Meier curves for overall survival in all PDAC patients or non-squamous subtype PDAC patients (I) from ICGC dataset stratified by YAP1 activation signature score. (J) YAP1 signature score in squamous (SQ) or progenitor (Pro) subtype human PDAC cell lines or PDXs (K). Error bars from all panels indicate ±SD. *: $p<0.05$; **: $p<0.01$. p value for survival analysis was calculated with log rank test.

Figure 3. YAP1 is essential for the maintenance of squamous subtype PDACs

(A) Representative images of the colony formation assay in human PDAC cell lines infected with YAP1 shRNAs or non-targeting shRNA (shCtr). The YAP1 knockdown efficiency was detected by Western blot. Quantification from triplicates is shown in (B) and is presented as relative colony numbers upon normalization to shCtr group. (C) Representative images of the colony formation assay in PDX cells infected with YAP1 shRNAs or non-targeting shRNA (shCtr). Quantification of from triplicates is shown in (D). (E) Representative images of the cell growth assay in human PDAC cell lines infected with YAP1 shRNAs or non-targeting shRNA (shCtr). Quantification from triplicates is shown in (F) and is presented as relative growth upon normalization to shCtr group. (G) KRAS-independence signature score among human PDAC subtypes. SQ: squamous subtype; Pro: progenitor subtype; ADEX: aberrantly differentiated endocrine exocrine subtype; Immu: immunogenic subtype. (H) YAP1 signature score among mouse PDAC tumours with indicated genotypes. (I) Representative images of the colony formation assay in mouse PDAC cells infected with Yap1 shRNAs or non-targeting shRNA (shCtr). Quantification of colony formation from triplicates is shown in (J). Error bars from all panels indicate ±SD. *: $p<0.05$; **: $p<0.01$.

Figure 4. YAP1 activation in PDAC is mediated by WNT5A overexpression

bioRxiv preprint doi: https://doi.org/10.1101/270314; this version posted February 23, 2018. The copyright holder for this preprint (which was not certified by peer review) is the author/funder. All rights reserved. No reuse allowed without permission.

(A) Human pancreatic cancer cell lines of progenitor or squamous subtype or mouse PDAC cells of indicated genotypes (B) were subjected to immunofluorescence staining with anti-YAP1 (red) and DAPI (blue). (C) Non-canonical (NC) WNT pathway enrichment score in iKras- mouse PDAC tumours without (Amp-) or with (Amp+) *Yap1* amplification. (D) Correlation between non-canonical WNT signature and YAP1 signature in PDAC TCGA dataset. (E) *WNT5A* expression in squamous (SQ) or progenitor (Pro) subtype human PDACs in TCGA dataset. (F) Western blots for WNT5A in mouse PDAC cells of indicated genotypes and human PDAC cell lines. (G) Western blot analysis for WNT5A, YAP1 and phospho-YAP1 (S127) in two independent *iKras-Yap1*$^{Amp-}$ cells with CRISPR-mediated *Wnt5a* deletion. Two independent *Wnt5a* knockout (KO) clones were included and clone without *Wnt5a* deletion was used as control (Ctr). (H) *iKras-Yap1*$^{Amp-}$*-Wnt5a* KO cells were subjected to immunofluorescence staining with anti-YAP1 (red) and DAPI (blue). (I) Relative mRNA levels of YAP1 downstream targets in *iKras-Yap1*$^{Amp-}$*-Wnt5a* KO cells. (J) Western blot analysis for WNT5A, YAP1 and phospho-YAP1 (S127) in mouse iKras PDAC cells or human PaTu8988S cells expressing GFP or WNT5A (Top). The quantification of phosphor-YAP1/total YAP1 signals is shown in the bottom panel. (K) PaTu8988S cells expressing GFP or WNT5A were subjected to immunofluorescence staining with anti-YAP1 (red) and DAPI (blue). (L) Western blot analysis for WNT5A, YAP1 and phospho-YAP1 (S127) in PaTu8988S cells infected with WNT5A shRNAs or non-targeting shRNA (shCtr). Error bars from all panels indicate ±SD. *: $p<0.05$; **: $p<0.01$. Scale bar: 20 μm.

Figure 5. WNT5A overexpression is required for tumourigenic activity

(A) Representative images of the colony formation assay for *iKras-Yap1*$^{Amp-}$-Wnt5a KO cells. Clones without *Wnt5a* deletion was used as control (Ctr). Quantification from triplicates is shown in (B) and is presented as relative colony numbers upon normalization to shCtr group. (C) Representative images of the colony formation assay in mouse PDAC cells of indicated genotypes treated with vehicle (DMSO)

bioRxiv preprint doi: https://doi.org/10.1101/270314; this version posted February 23, 2018. The copyright holder for this preprint (which was not certified by peer review) is the author/funder. All rights reserved. No reuse allowed without permission.

or WNT5A antagonist, BOX5 (100μM). Quantification from triplicates is shown in (D) and is presented as relative colony numbers upon normalization to DMSO group. (E) Two independent clones of *iKras-Yap1*$^{Amp-}$*-Wnt5a* KO cells and control cells without *Wnt5a* deletion (CTR) were subcutaneously injected into nude mice. Tumour volumes were measured on the indicated dates post-injection. Results are presented as the means±SEM. (n=6). (F) *iKras- Yap1*$^{Amp-}$*-Wnt5a* KO cells were infected with GFP, WNT5A or YAP1^{S127A} and were subcutaneously injected into nude mice. Cells without *Wnt5a* deletion were used as control (CTR). Tumour volumes were measured 30 days post-injection. Results are presented as the means±SEM. (n=6). (G) Subcutaneous xenograft tumours from (E) were stained for YAP1 (Scale bar: 100 μm.). Percentage of cells with nuclear/cytoplasmic/double staining of YAP1 is shown in (H). Error bars represent SD (n=10 fields, 250 celss/field), (I) Representative images of the colony formation assay for PaTu8988T cells infected with WNT5A shRNAs or non-targeting shRNA (shCtr) (top). Quantification from triplicates is shown in the bottom panel. Error bars from all panels indicate ±SD. *: $p<0.05$; **: $p<0.01$.

Figure 6. WNT5A overexpression leads to the bypass of KRAS-dependency

(A) Cell growth assay for PaTu8988S-GFP or –WNT5A cells infected with KRAS shRNAs or non-targeting control shRNA. Quantification from triplicates is presented as relative cell growth upon normalization to control group. Error bars indicate ±SD of triplicates, **: $p<0.01$. (B) Western blot analysis for WNT5A and YAP1 in mouse iKras tumour cells expressing GFP or WNT5A upon knockdown of YAP1 with shRNA. (C) Tumour sphere assay for mouse iKras-GFP or -WNT5A cells infected with non-targeting shRNA or YAP1 shRNA in the presence or absence of doxycycline. Representative images show the FACS analysis of annexin V and 7AAD staining. Numbers represent the percentage of early apoptosis (Annexin V^+ $7AAD^-$) and late apoptosis (Annexin V^+ $7AAD^+$) populations with quantification shown in (D). Error bars indicate SD of replicates. *: $p<0.05$; **: $p<0.01$.

bioRxiv preprint doi: https://doi.org/10.1101/270314; this version posted February 23, 2018. The copyright holder for this preprint (which was not certified by peer review) is the author/funder. All rights reserved. No reuse allowed without permission.

(E) Schematic workflow for the in vivo Kras bypass experiment. (F) Mouse iKras tumour cells expressing luciferase were infected with lentivirus expressing GFP, WNT5A or YAP1^{S127A} and orthotopically injected into nude mice pancreas. Animals were kept off doxycycline and tumour growth was visualized by bioluminescent imaging at 8 weeks. (G) Kaplan-Meier overall survival analysis for nude mice (n=5/group) orthotopically transplanted with the cells described in (F). (H) Orthotopic xenograft tumours generated with iKras-GFP cells (on doxycycline) or iKras-WNT5A cells (off doxycycline) were stained for WNT5A, YAP1 and phospho-ERK (Scale bar: 100 μm.).

Figure 7. WNT5A-YAP1 axis is active in primary human PDAC and required for tumour maintenance

(A) *WNT5A* expression in squamous (SQ) or progenitor (Pro) subtype PDXs. (B) Correlation between *WNT5A* expression level and YAP1 activation signature in PDXs. (C) Correlation between *WNT5A* expression and YAP1 signature in PDAC TCGA dataset. (D) Western blot analysis for WNT5A, YAP1, phospho-YAP1 (S127) and CYR61 in PDX cell lines of squamous or progenitor subtype. (E) Western blot analysis for WNT5A, YAP1 and phospho-YAP1 (S127) in squamous subtype PDX cell lines infected with WNT5A shRNAs or non-targeting shRNA (shCtr). (F) Representative images of the colony formation assay for squamous subtype PDX cell lines infected with WNT5A shRNAs or non-targeting shRNA (shCtr). Quantification from triplicates is shown in (G). (H) PATC148 cells infected with WNT5A shRNAs or non-targeting shRNA (shCtr) were subcutaneously injected into nude mice. Tumour volumes were measured on the indicated dates post-injection. Results are presented as the means±SEM. (n=6). (I) Western blot analysis for KRAS, phosphor-MEK1/2 and MEK1/2 in PDX cell lines infected with KRAS shRNAs or non-targeting shRNA (shCtr). (J) Cell growth assay for PDX cell lines infected with KRAS shRNAs or non-targeting shRNA (shCtr). Quantification from triplicates is

bioRxiv preprint doi: https://doi.org/10.1101/270314; this version posted February 23, 2018. The copyright holder for this preprint (which was not certified by peer review) is the author/funder. All rights reserved. No reuse allowed without permission.

presented as relative cell growth upon normalization to shCtr group. Error bars from all panels indicate ±SD. *: $p<0.05$; **: $p<0.01$.

bioRxiv preprint doi: https://doi.org/10.1101/270314; this version posted February 23, 2018. The copyright holder for this preprint (which was not certified by peer review) is the author/funder. All rights reserved. No reuse allowed without permission.

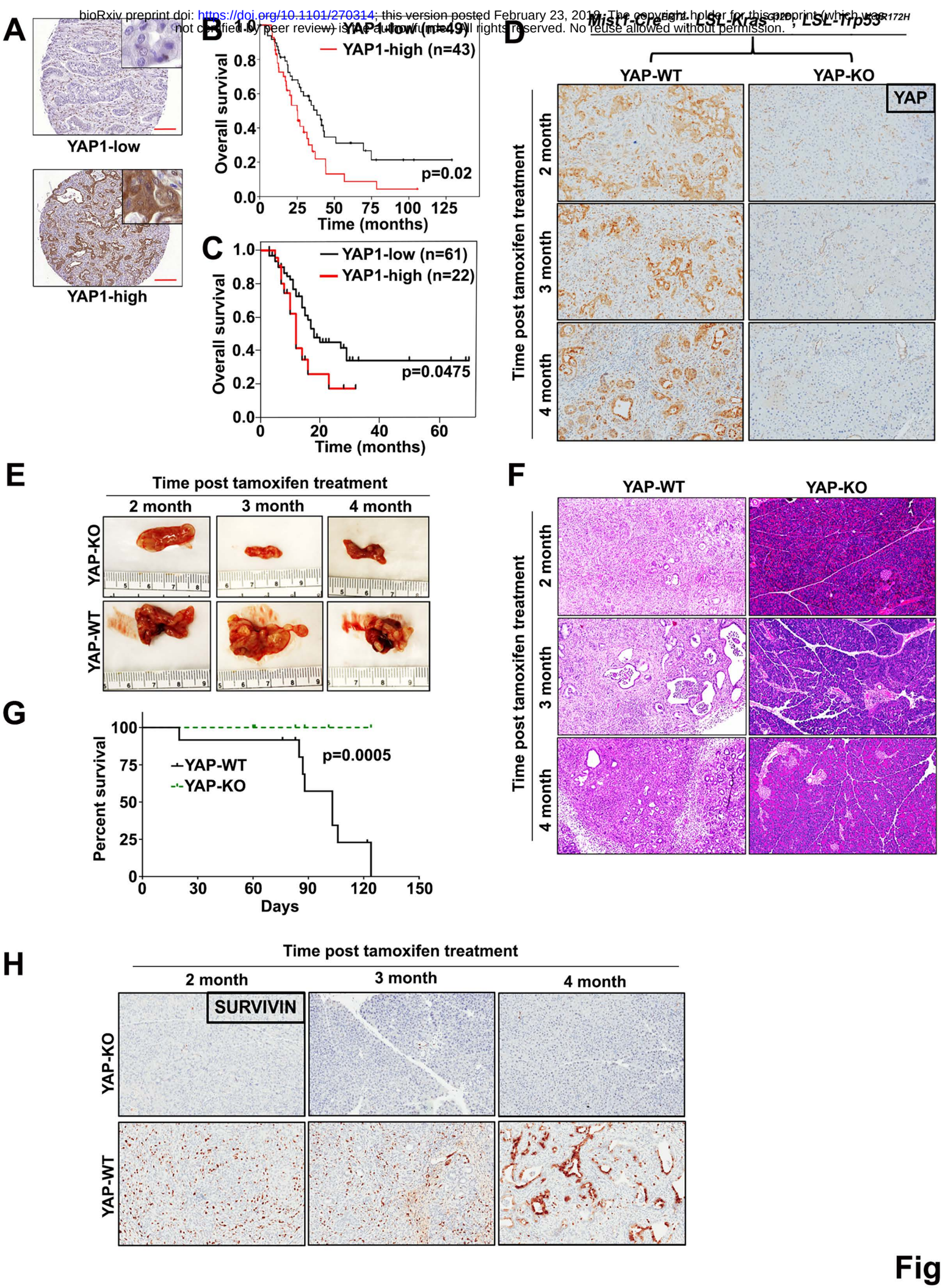

Fig.1

bioRxiv preprint doi: https://doi.org/10.1101/270314; this version posted February 23, 2018. The copyright holder for this preprint (which was not certified by peer review) is the author/funder. All rights reserved. No reuse allowed without permission.

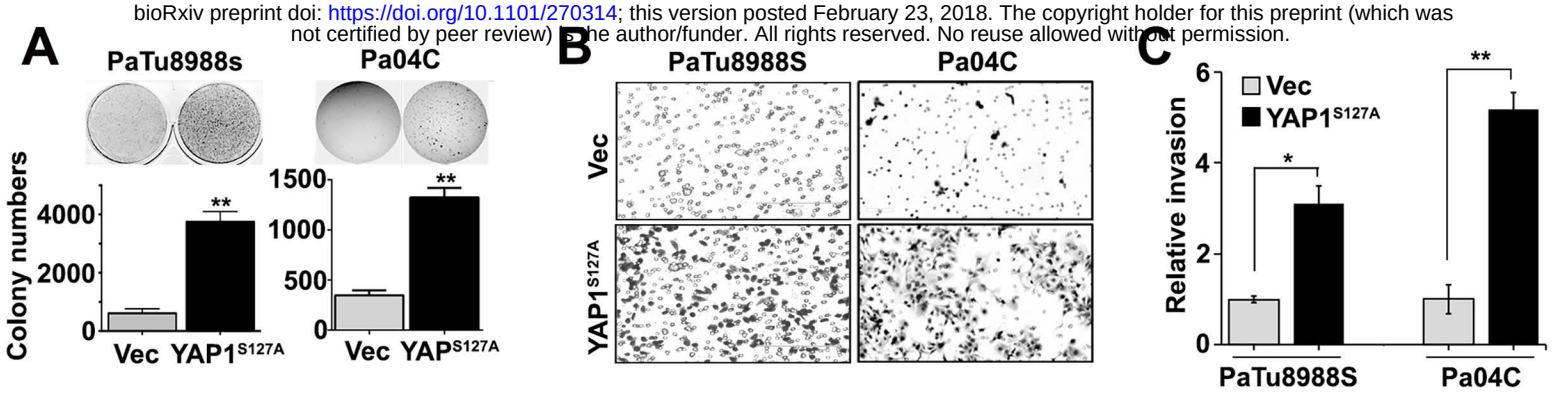

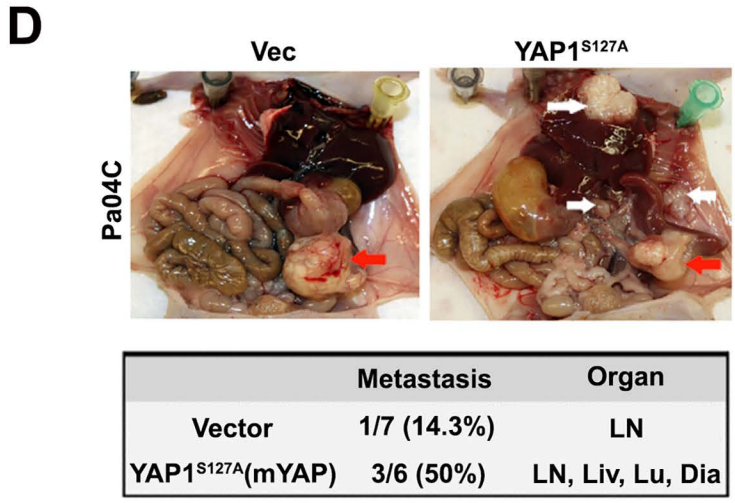

	Metastasis	Organ
Vector	1/7 (14.3%)	LN
YAP1S127A(mYAP)	3/6 (50%)	LN, Liv, Lu, Dia

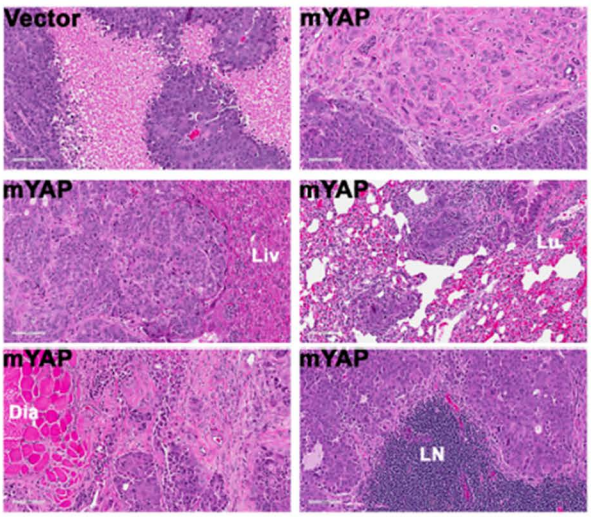

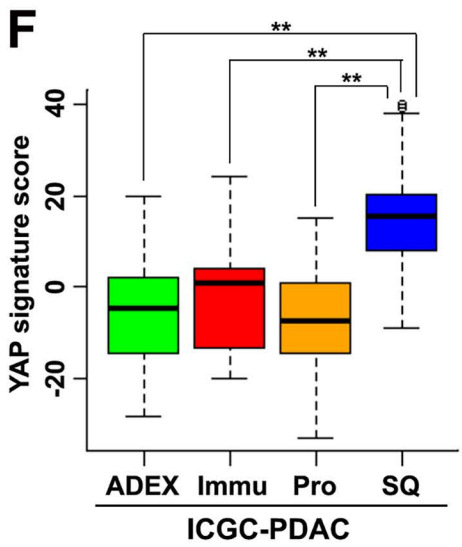

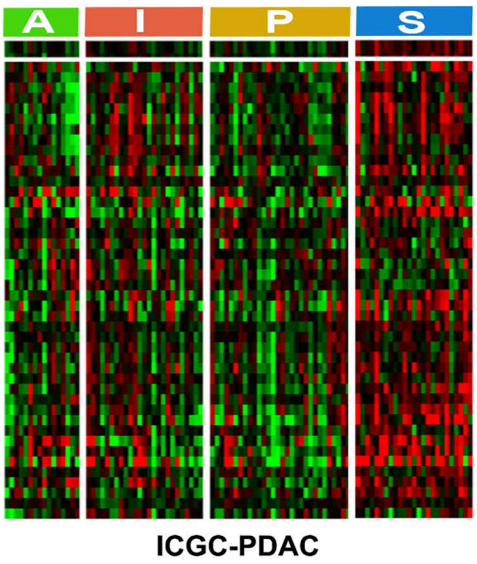

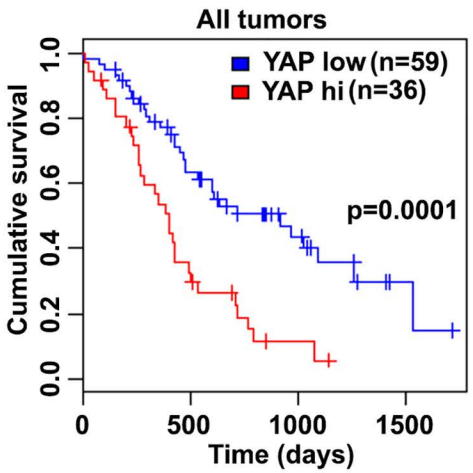

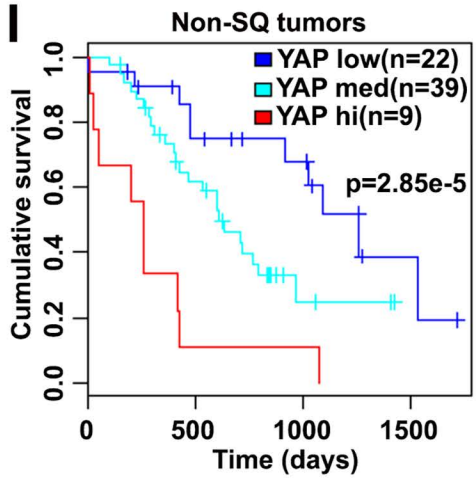

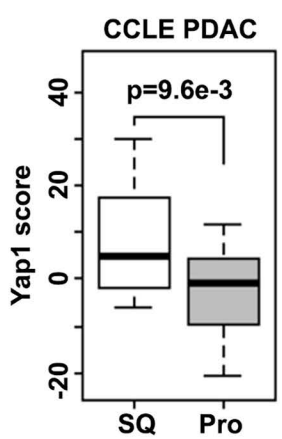

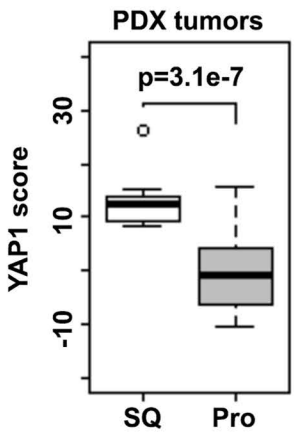

Fig.2

bioRxiv preprint doi: https://doi.org/10.1101/270314; this version posted February 23, 2018. The copyright holder for this preprint (which was not certified by peer review) is the author/funder. All rights reserved. No reuse allowed without permission.

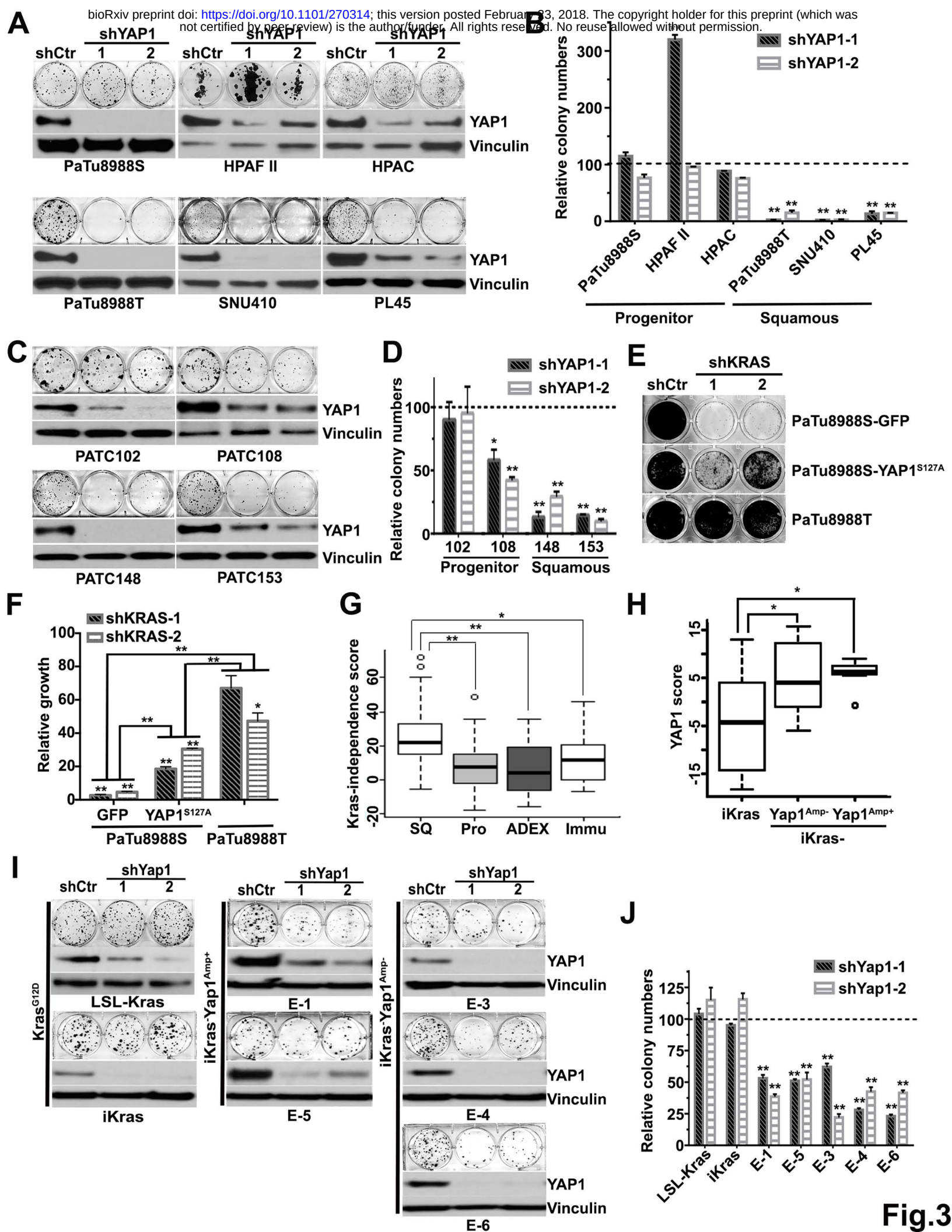

Fig.3

bioRxiv preprint doi: https://doi.org/10.1101/2020.02.23.961540; this version posted February 23, 2020. The copyright holder for this preprint (which was not certified by peer review) is the author/funder. All rights reserved. No reuse allowed without permission.

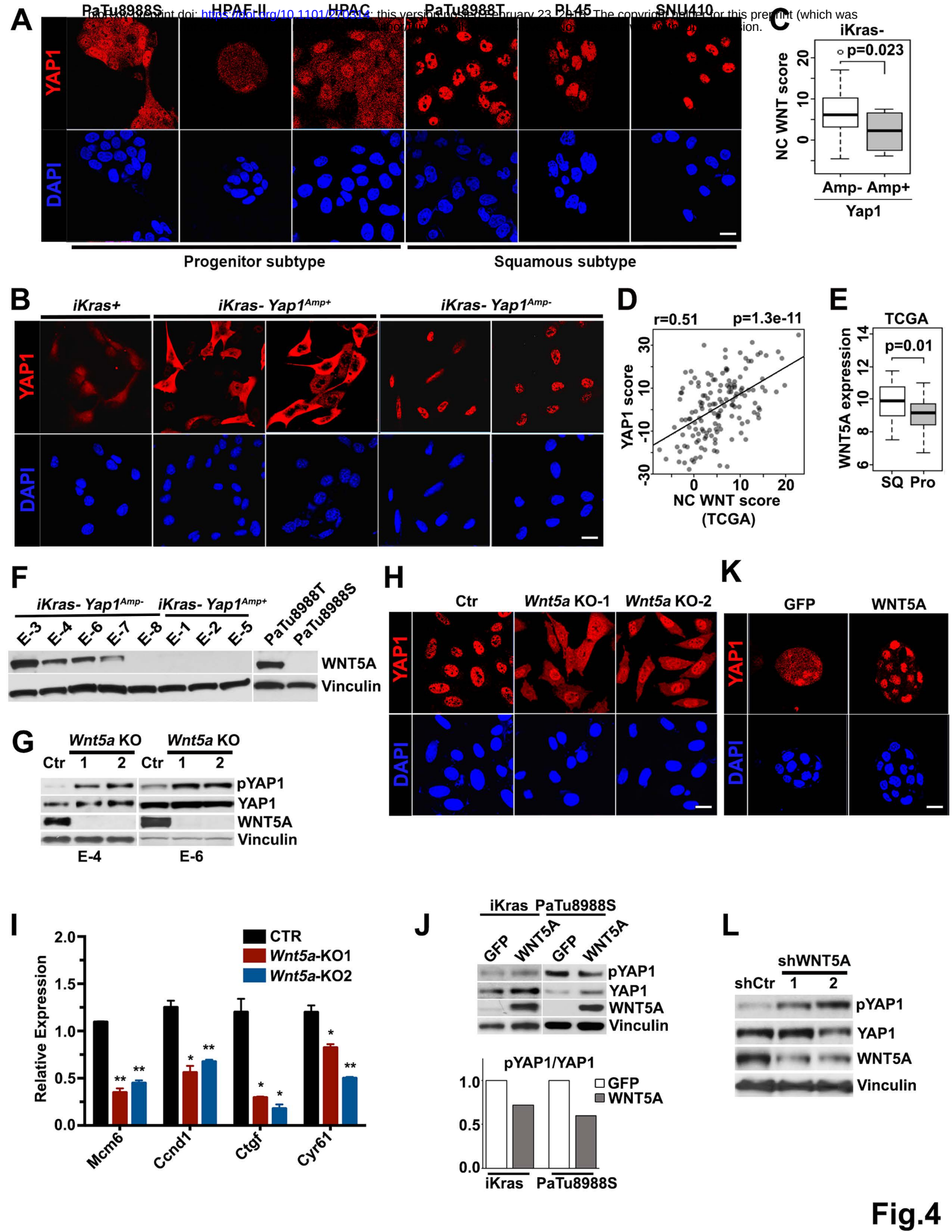

Fig.4

bioRxiv preprint doi: https://doi.org/10.1101/270314; this version posted February 23, 2018. The copyright holder for this preprint (which was not certified by peer review) is the author/funder. All rights reserved. No reuse allowed without permission.

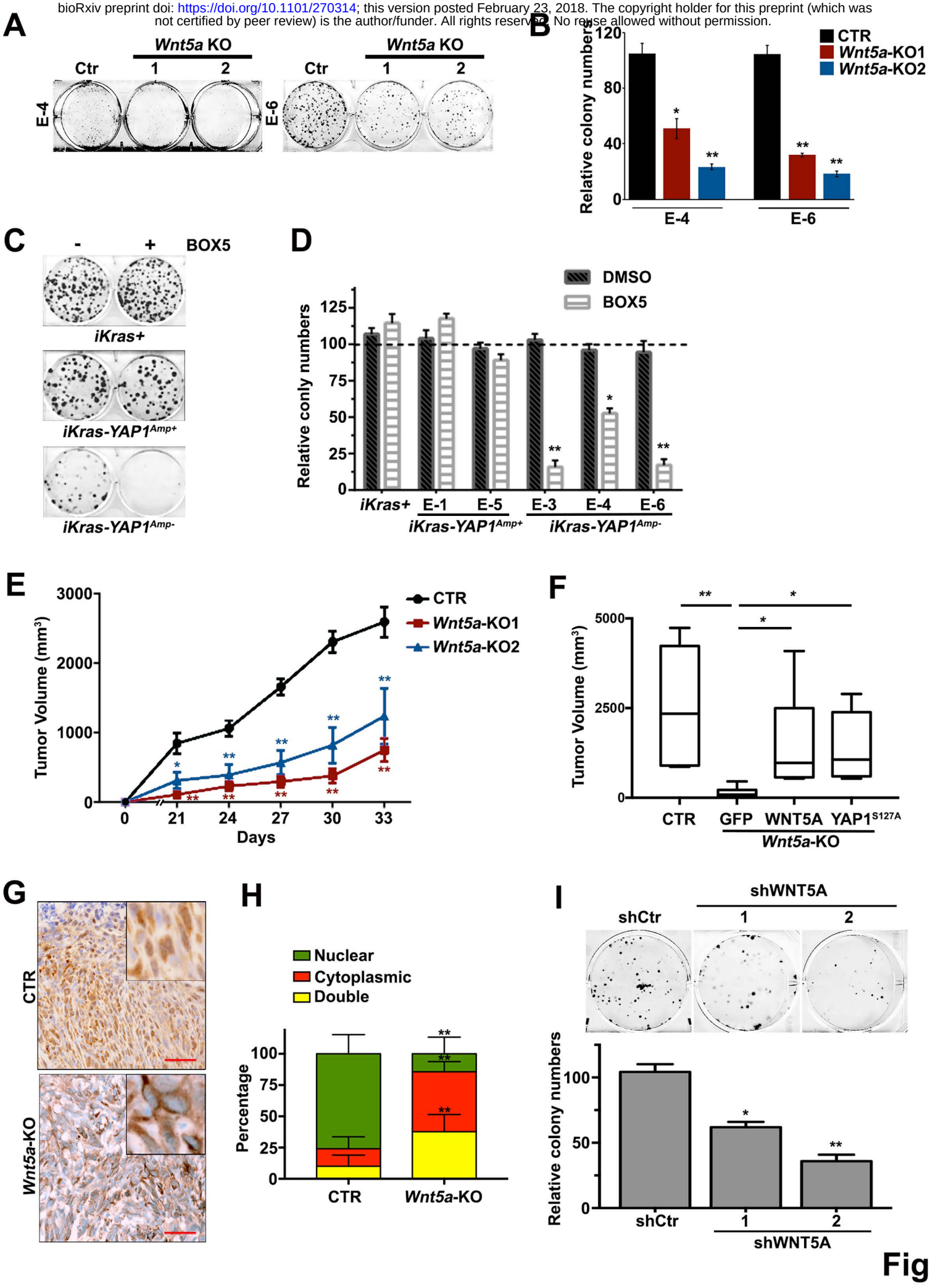

Fig.5

bioRxiv preprint doi: https://doi.org/10.1101/270314; this version posted February 23, 2018. The copyright holder for this preprint (which was not certified by peer review) is the author/funder. All rights reserved. No reuse allowed without permission.

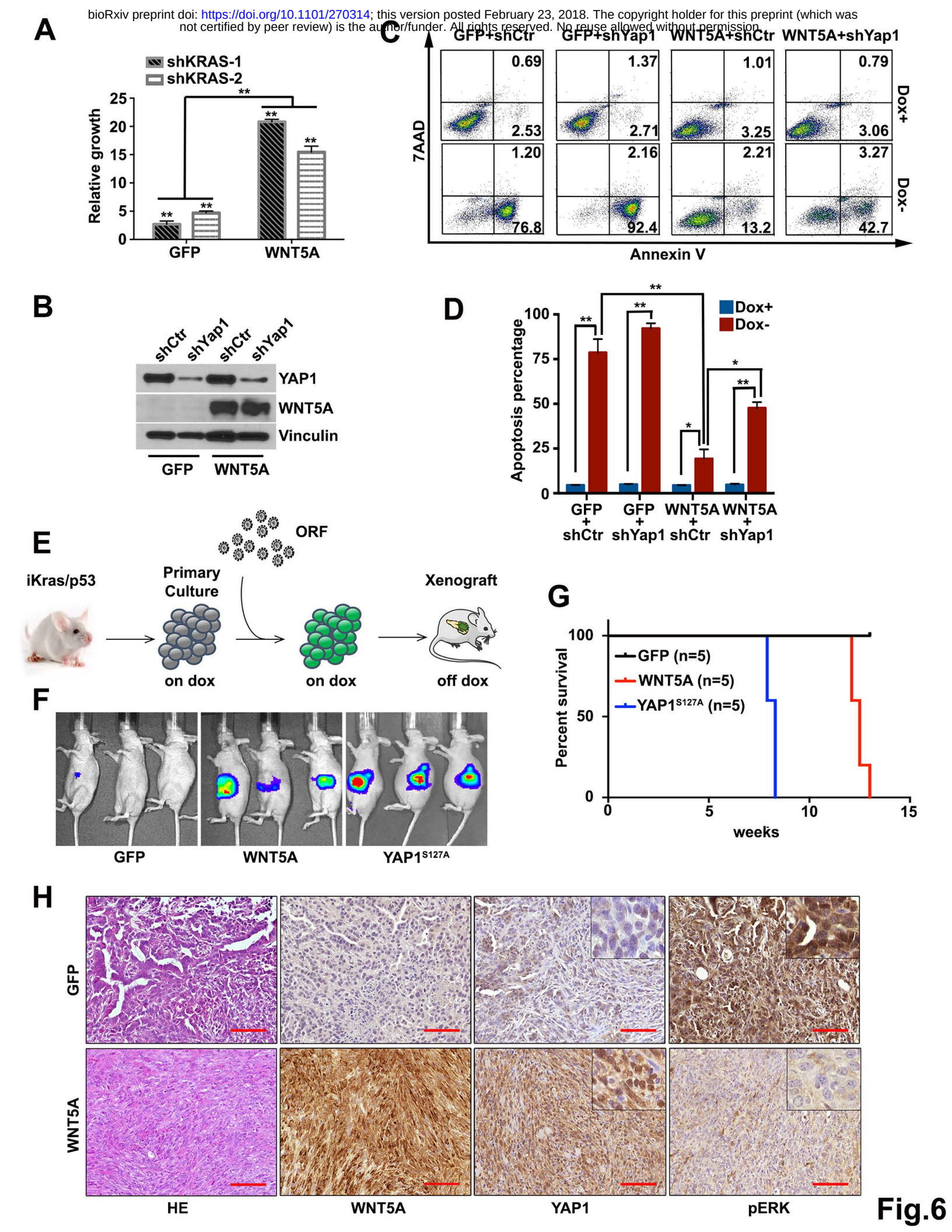

Fig.6

bioRxiv preprint doi: https://doi.org/10.1101/270314; this version posted February 23, 2018. The copyright holder for this preprint (which was not certified by peer review) is the author/funder. All rights reserved. No reuse allowed without permission.

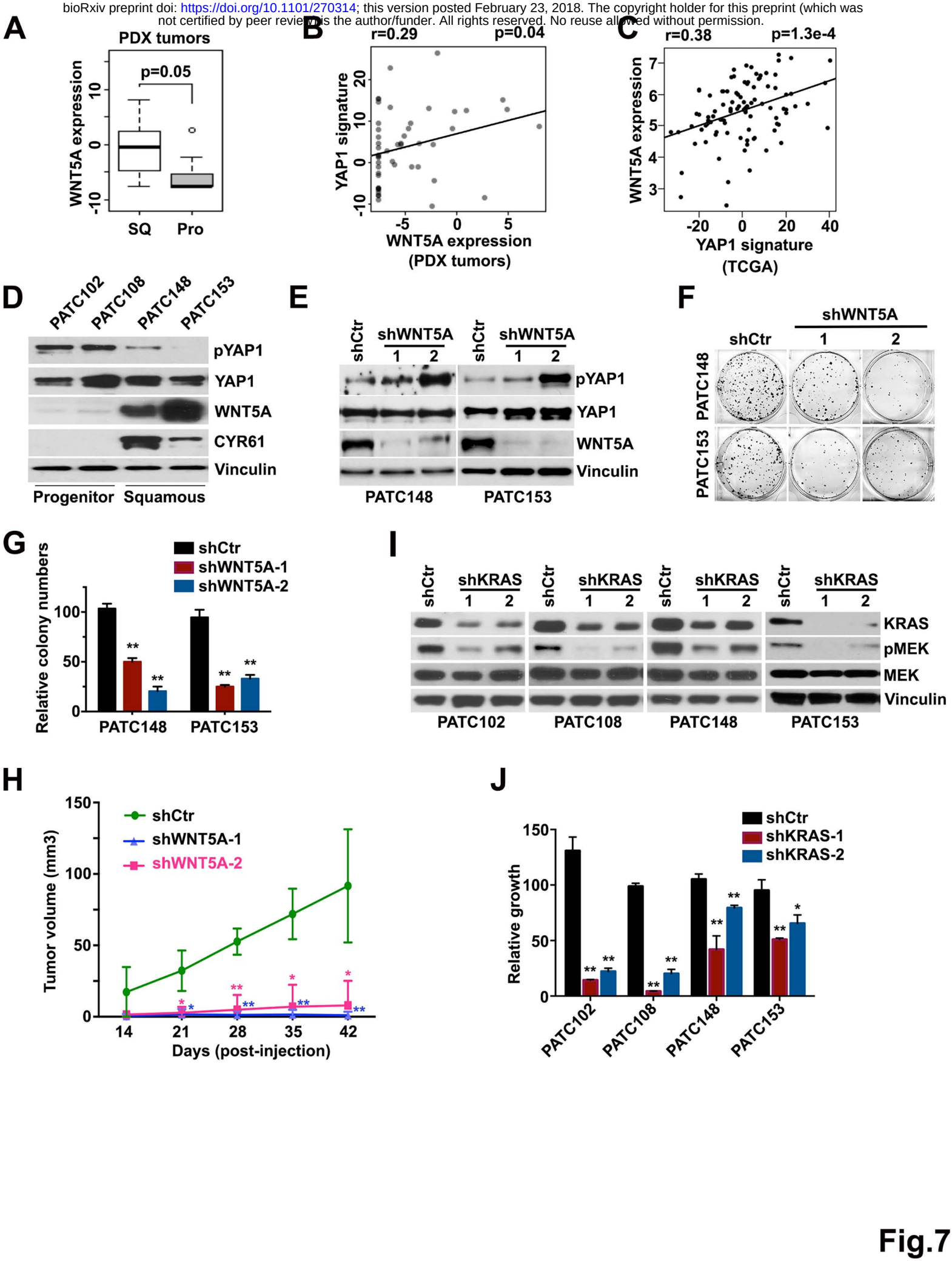

Fig.7

bioRxiv preprint doi: https://doi.org/10.1101/270314; this version posted February 23, 2018. The copyright holder for this preprint (which was not certified by peer review) is the author/funder. All rights reserved. No reuse allowed without permission.

Supplementary Materials and Method

Immunostaining and Western Blot Analysis

For immunofluorescence staining, mouse and human cells were fixed with 4% paraformaldehyde-PBS for 15 min. Following Triton-X100 permeabilization and blocking, cells were incubated with primary antibodies overnight at 4°C following with Alexa 594-conjugated secondary antibodies at 4°C for 1 hour (Thermo Fisher Scientific, 1:1000). Samples were mounted using VECTASHIELD Antifade Mounting Medium with DAPI (Vector Laboratories) and immunofluorescence was detected using Olympus confocal microscopy. For western blot analysis, cells were lysed on ice using RIPA buffer supplemented with protease and phosphatase inhibitors (Sigma).

Primary Antibodies for Immunostaining and Western Blot Analysis: Yap (#14074, Cell Signaling), pYAP (#4911, Cell Signaling), Lats1 (#3477, Cell Signaling), pLats1(#8654, Cell Signaling), Mst1 (#3682, Cell Signaling), Mst2 (#3952,Cell Signaling), p-MST1/2 (#3681, Cell Signaling), Merlin(#12888, Cell Signaling), Phospho-Merlin (#13281,Cell Signaling), Wnt5a (#2530, Cell Signaling), Ki-67 (VP-K451, Vector Laboratories), Cyr61 (sc-13100, Santa Cruz Biotechnology), CTGF (sc-14939, Santa Cruz Biotechnology), AXL (8661, Cell Signaling), pErk (4376, Cell Signaling), pMEK (4376, Cell Signaling), Ck-19 (16858-1-AP, Proteintech), Actin (A2228, Sigma Aldrich), Vinculin (V4139, Sigma Aldrich), Kras (sc-30, Santa Cruz Biotechnology).

Lentivirus Mediated shRNA Knockdown

The clone IDs for shRNA are as follows: sh_mouse Yap1-1 (TRCN0000238436), sh mouse Yap1-2 (TRCN0000095864), sh_huYap1-1 (TRCN0000107265), sh_huYap1-2

bioRxiv preprint doi: https://doi.org/10.1101/270314; this version posted February 23, 2018. The copyright holder for this preprint (which was not certified by peer review) is the author/funder. All rights reserved. No reuse allowed without permission.

(TRCN0000107266), sh_huWnt5a-1 (TRCN0000062717), sh_huWnt5a-2 (TRCN0000288987), sh_hu Kras-1 (TRCN0000033260), sh_hu Kras-2 (TRCN0000033262).

Crispr-Cas9 Mediated Gene Knockout

Sequences for Wnt5a sgRNA are as follows:

sgRNA-1 F: CTTGAGAAAGTCCTGCCAGT; R: ACTGGCAGGACTTTCTCAAG.

sgRNA-2 F: GAAACTCTGCCACTTGTATC; R: GATACAAGTGGCAGAGTTTC.

sgRNA-3 F: TATACTTCTGACATCTGAAC; R: GTTCAGATGTCAGAAGTATA.

sgRNA-4 F: ACAGCCTCTCTGCAGCCAAC, R: GTTGGCTGCAGAGAGGCTGT.

Xenograft Studies

For orthotopic xenografts, 5×10^5 cells were injected pancreatically into NCr nude mice (Taconic) and tumor growth was monitored with bioluminescent imaging as described [1]. For Sub-Q xenografts, 1×10^6 cells (mouse tumor cells) or 3×10^6 cells (human PDX cells) were injected subcutaneously into the lower flank of NCr nude mice. Tumor volumes were measured every 7 days starting from Day 7 post injection and calculated using the formula, volume = length $\times$ width^2/2.

Immunoprecipitation Assay

Immunoprecipitation of YAP1 complexes was performed by lysing cells with 1% NP40 lysis buffer containing phosphatase and protease inhibitor cocktails on ice for 45 minutes. 1 mg of lysate was incubated overnight at 4^{o}C with primary antibodies followed with protein A/G Plus-agarose (sc-2003, Santa Cruz) for 3 hours at 4^{o}C. Immunoprecipitates were washed three times with lysis buffer, then re-suspended with 2X sample buffer boiled for 5 min and detected by western blot analyses.

Quantitative Real-time Polymerase Chain Reaction Analysis

bioRxiv preprint doi: https://doi.org/10.1101/270314; this version posted February 23, 2018. The copyright holder for this preprint (which was not certified by peer review) is the author/funder. All rights reserved. No reuse allowed without permission.

RNA from cell lines and pancreas tissues was isolated using RNeasy Mini Kit (Qiagen) and first-strand cDNA was synthesized from 2 µg total RNA using random primers and Omniscript® Reverse Transkriptase Kit (Qiagen). Actin was used as housekeeping gene. Real-time polymerase chain reaction experiments were performed in triplicates and are displayed ± SD.

Clonogenic assay

500-2000 cells were seeded into each well of 6-well plate in triplicates and incubated to allow colony formation for 10-20 days. The colonies were stained with 0.2% crystal violet in 80% methanol for 30 minutes at room temperature and de-stained upon which they were scanned and colonies counted using Image J (http://rsb.info.nih.gov/ij/).

Gene Expression and PDAC-Subtype Analysis

mRNA expression profiling was performed using the Mouse Genome 430 2.0 Array (Affymetrix). To identify differentially enriched gene sets, the raw intensities were log2-transformed and quantile normalized. The software package LIMMA (Linear Models for Microarray Data) was applied to detect significantly differentially expressed probes using Benjamini-Hochberg adjusted p-values. For GSEA analysis, gene sets collection from MSigDB 3.0 and Kyoto Encyclopedia of Genes and Genomes (KEGG) were included in the analysis.

For PDAC-subtype analysis, data generated from Affymetrix arrays was preprocessed using Robust Multi-array (RMA) algorithm using R-based bioconductor. The replicates from each array were averaged. A reduced set of PDAssigner genes[2] (49 out of 62) were mapped to this data set and simple hierarchical clustering using Cluster 3.0[3] was performed to assign these cells to PDAssigner subtypes. The clusters were viewed using Java TreeView (version 1.1.6r4, [4]).

bioRxiv preprint doi: https://doi.org/10.1101/270314; this version posted February 23, 2018. The copyright holder for this preprint (which was not certified by peer review) is the author/funder. All rights reserved. No reuse allowed without permission.

Supplementary Reference

1. Kapoor A, Yao W, Ying H, et al. Yap1 activation enables bypass of oncogenic Kras addiction in pancreatic cancer. *Cell* 2014;158(1):185-97. doi: 10.1016/j.cell.2014.06.003 [published Online First: 2014/06/24]
2. Collisson EA, Sadanandam A, Olson P, et al. Subtypes of pancreatic ductal adenocarcinoma and their differing responses to therapy. *Nat Med* 2011;17(4):500-3. doi: 10.1038/nm.2344 [published Online First: 2011/04/05]
3. Eisen MB, Spellman PT, Brown PO, et al. Cluster analysis and display of genome-wide expression patterns. *Proc Natl Acad Sci U S A* 1998;95(25):14863-8.
4. Saldanha AJ. Java Treeview--extensible visualization of microarray data. *Bioinformatics* 2004;20(17):3246-8. doi: 10.1093/bioinformatics/bth349

bioRxiv preprint doi: https://doi.org/10.1101/270314; this version posted February 23, 2018. The copyright holder for this preprint (which was not certified by peer review) is the author/funder. All rights reserved. No reuse allowed without permission.

Supplementary Figure Legends

Figure S1. YAP1 is essential for PDAC development.

(A) *Yap1* wild-type (YAP-WT) or knockout (YAP-KO) *Kras*^{G12D};*Trp53*^{R172H} mice driven by *Mist1-Cre*^{ERT2} upon tamoxifen injection. Pacreata were collected at indicated time points and stained for Ki-67 to assess cell proliferation. (B) *Yap1* wild-type (YAP-WT) or knockout (YAP-KO) *Kras*^{G12D};*Trp53*^{R172H} mice driven by *Elastase-Cre*^{ERT2} upon tamoxifen injection. Pacreata collected at 4 months post-injection and stained for H&E (Top) shows complete block of tumor development and relative normal pancreatic architecture in YAP-KO mice in contrast with ductal adenocarcinoma in YAP-WT mice. (Bottom) Immunostaining for YAP shows strong nuclear staining in tumor epithelia of YAP-WT pancreata while showing complete lack of expression in YAP-KO mice.

Figure S2. YAP1 enhances the malignant phenotypes of PDAC and is activated in squamous subtype.

(A) In vitro wound healing assay for Pa04C cells expressing YAP1^{S127A} or control vector (Vec) showing more aggressive migration of Pa04C-YAP1^{S127A} cells. (B) Orthotopic xenograft tumors from Pa04C cells expressing vector (Vec) or YAP1^{S127A} were stained for known YAP1-target genes CYR61, CTGF and AXL. (C) GSEA plot of YAP1 activation signature based on the gene expression profiles of vector- vs YAP1^{S127A}-expressing Pa04C cells. NES denotes normalized enrichment score. (D) Relative mRNA levels of *YAP1* and indicated YAP1-target genes in Pa04C cells expressing vector (Vec) or YAP1^{S127A}. Error bars indicate ±SD of triplicates. **: $p<0.01$. (E) -(G) GSEA plot of multiple metastasis (E), cell migration and cell motility (F) and EMT (G) pathways based on the gene expression profiles of vector- vs YAP1^{S127A}-expressing Pa04C cells. NES denotes normalized enrichment score. (H) Relative mRNA levels of indicated

bioRxiv preprint doi: https://doi.org/10.1101/270314; this version posted February 23, 2018. The copyright holder for this preprint (which was not certified by peer review) is the author/funder. All rights reserved. No reuse allowed without permission.

EMT genes in Pa04C cells expressing vector (Vec) or YAP1^{S127A}. Error bars indicate ±SD of triplicates. **: p<0.01. (I) Clustering of human PDAC cell lines based on subtype-specific gene signatures. Heatmap of squamous (SQ) and progenitor (PRO) subtype gene expression is shown. (J) Clustering of human PDXs based on subtype-specific gene signatures. Heatmap of squamous (SQ) and progenitor (PRO) subtype gene expression is shown. (K) Heatmap shows the expression level of squamous (SQ) and progenitor (PRO) subtype signature genes measured with Nanostring in PaTu8988S cells expressing GFP or YAP1^{S127A} and PaTu8988T cells.

Figure S3. YAP1 is activated squamous subtype PDACs.

(A) Western blot analysis for KRAS, phosphor-MEK1/2 and MEK1/2 in PaTu8988S cells expressing GFP or YAP1^{S127A} and PaTu8988T cells upon knockdown of KRAS with two independent shRNAs. Non-targeting shRNA (shCtr) was used as control. (B) & (C) GSEA plot of pathways induced upon KRAS knockdown in squamous subtype human PDAC from ICGC dataset. Heatmaps of signature gene expression among human PDAC subtypes are shown. (D) Heatmap shows the expression of KRAS-independence gene signature among human PDAC subtypes in ICGC dataset. S: squamous subtype; A: ADEX subtype; P: progenitor subtype; I: immunogenic subtype. (E) Two independent *iKras- Yap1*$^{Amp-}$ cell lines were infected with two independent shRNAs targeting Yap1 or non-targeting shRNA (shCtr). Cells were cultured in the presence or absence of doxycycline for 48 hours and cell lysates were subjected to western blot analysis for YAP1, phosphor-ERK and ERK. (F) Representative images of the colony formation assay upon Yap1 knockdown in *iKras- Yap1*$^{Amp-}$ cell lines grown in the presence or absence of doxycycline. Non-targeting shRNA (shCtr) was used as control. Quantification of colony formation is shown in (F) and is presented as relative colony numbers upon normalization to shCtr group. Error bars represent ±SD of triplicate wells, **: p<0.01.

bioRxiv preprint doi: https://doi.org/10.1101/270314; this version posted February 23, 2018. The copyright holder for this preprint (which was not certified by peer review) is the author/funder. All rights reserved. No reuse allowed without permission.

Figure S4. YAP1 activation in PDAC is mediated by WNT5A overexpression

(A) Mutation and copy number alteration (CAN) requency of *YAP1* in human PDAC from ICGC and TCGA datasets. (B) *Yap1* gene amplification status in *iKras*- tumors. (C) *iKras*+, *iKras*- *Yap1*$^{Amp-}$ and *iKras*- *Yap1*$^{Amp+}$ tumors were stained for YAP1. (D) Equal amount of YAP1 protein was immunoprecipitated from human PDAC cell lines of indicated subtypes and subjected to western blot analysis for phosphor-YAP1 (S127) and YAP1 (top). Input shows the western blot analysis for YAP1 in whole cell lysates (bottom). (E) Equal amount of YAP1 or LATS1/2 protein was immunoprecipitated from mouse *iKras*- PDAC cells and subjected to western blot analysis for phosphor-YAP1 (S127) and YAP1, or phosphor-LATS1/2 and LATS1/2 (top). Input shows the western blot analysis for phosphor-MST1/2, MST1, MST2, LATS1/2 and YAP1 in whole cell lysates (bottom). (F) Relative mRNA levels of indicated WNT ligands in mouse *iKras*- PDAC cells. Error bars indicate ±SD of triplicates.

bioRxiv preprint doi: https://doi.org/10.1101/270314; this version posted February 23, 2018. The copyright holder for this preprint (which was not certified by peer review) is the author/funder. All rights reserved. No reuse allowed without permission.

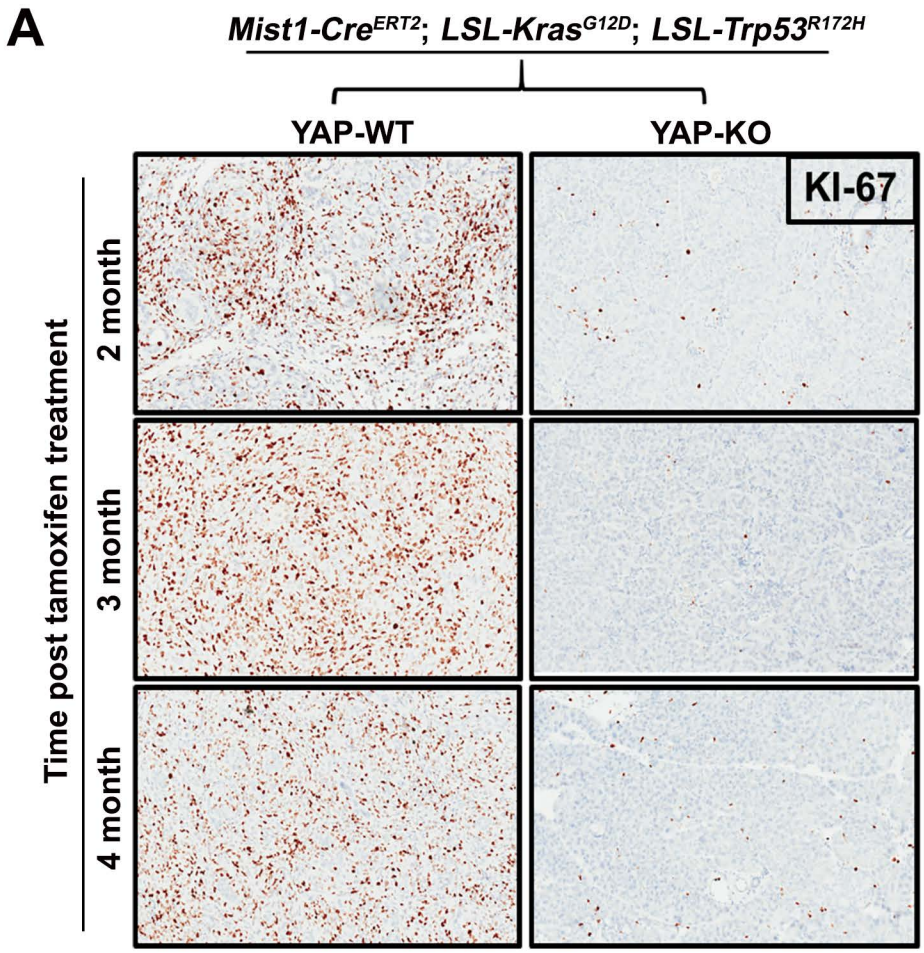

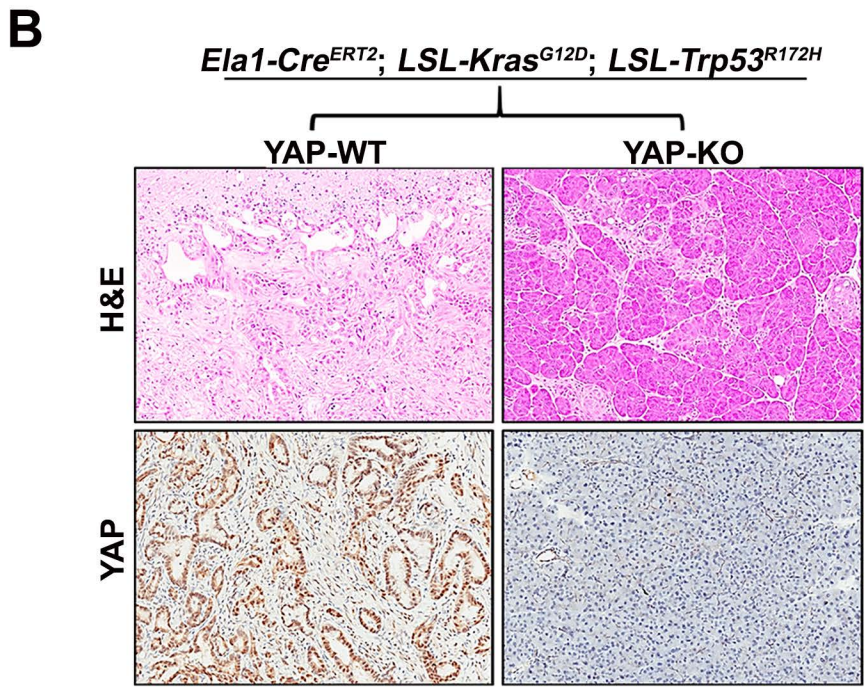

Fig. S1

bioRxiv preprint doi: https://doi.org/10.1101/270314; this version posted February 23, 2018. The copyright holder for this preprint (which was not certified by peer review) is the author/funder. All rights reserved. No reuse allowed without permission.

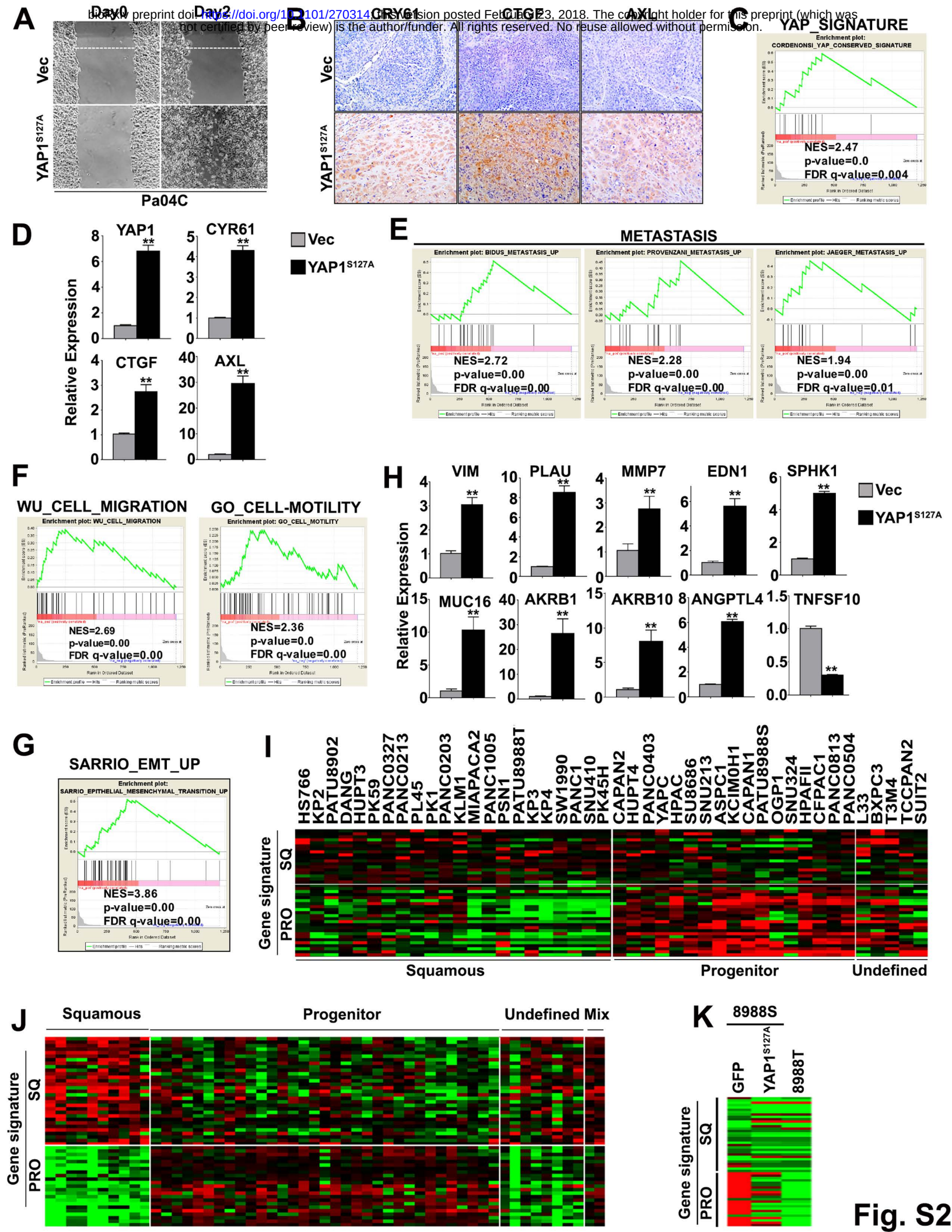

Fig. S2

bioRxiv preprint doi: https://doi.org/10.1101/270314; this version posted February 23, 2018. The copyright holder for this preprint (which was not certified by peer review) is the author/funder. All rights reserved. No reuse allowed without permission.

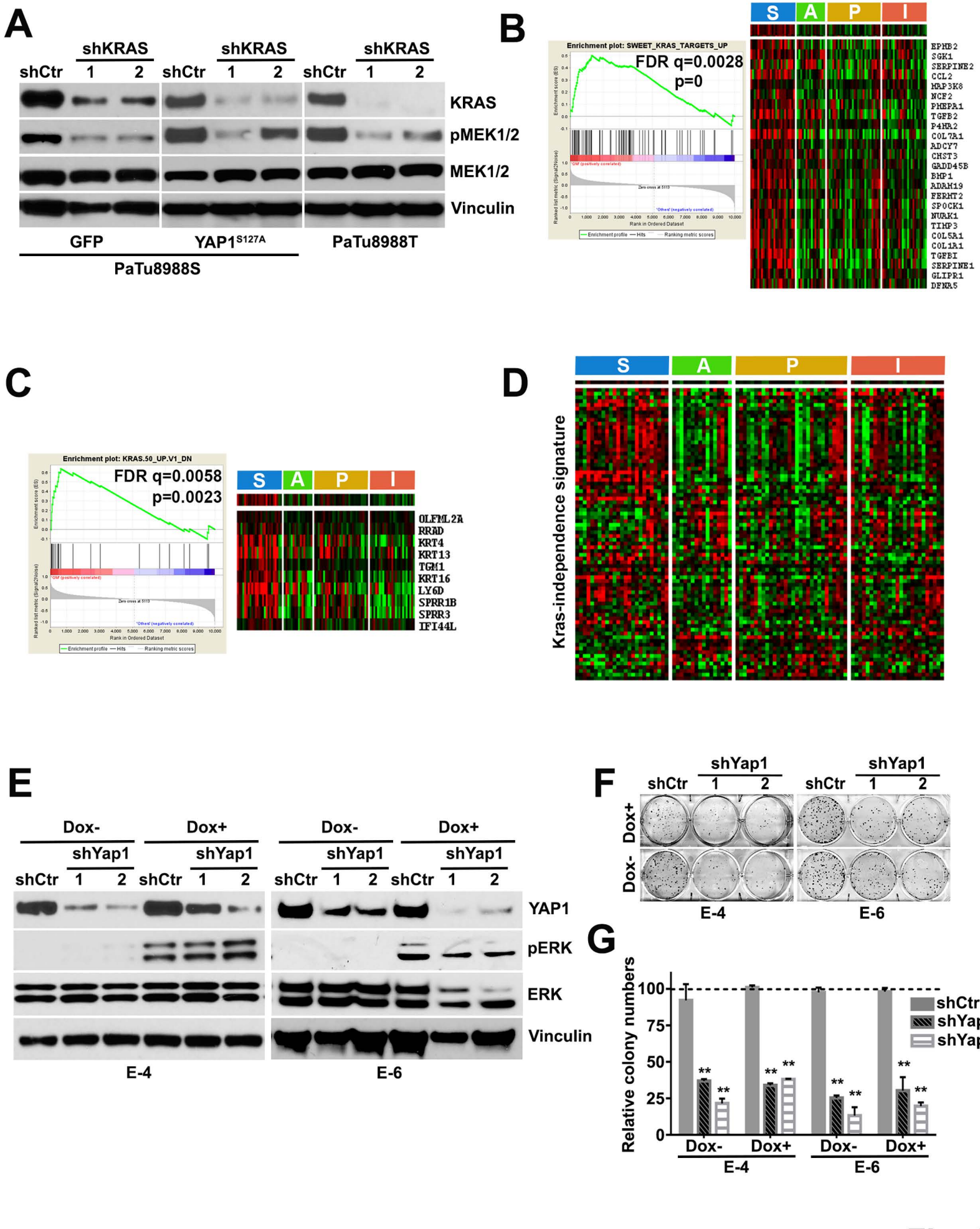

Fig. S3

bioRxiv preprint doi: https://doi.org/10.1101/270314; this version posted February 23, 2018. The copyright holder for this preprint (which was not certified by peer review) is the author/funder. All rights reserved. No reuse allowed without permission.

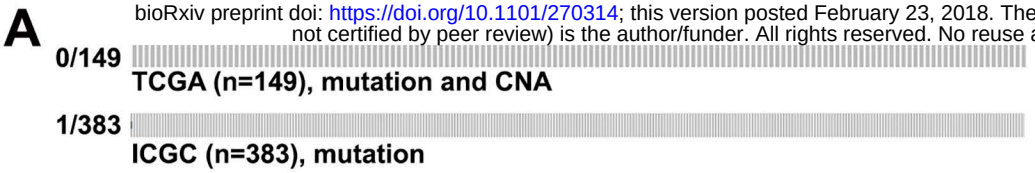

B

iKras-escapers	*Yap1* Amplification
E-1	+
E-2	+
E-3	-
E-4	-
E-5	+
E-6	-
E-7	-
E-8	-

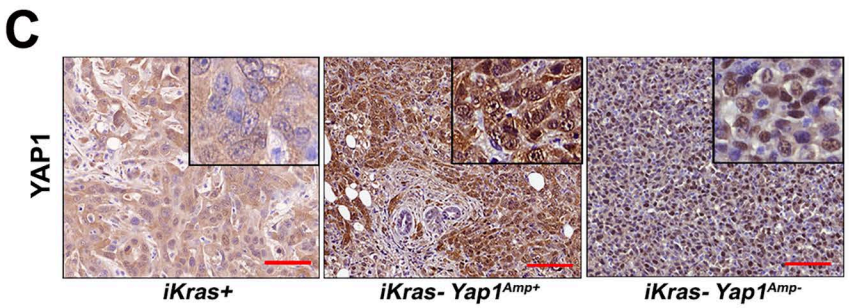

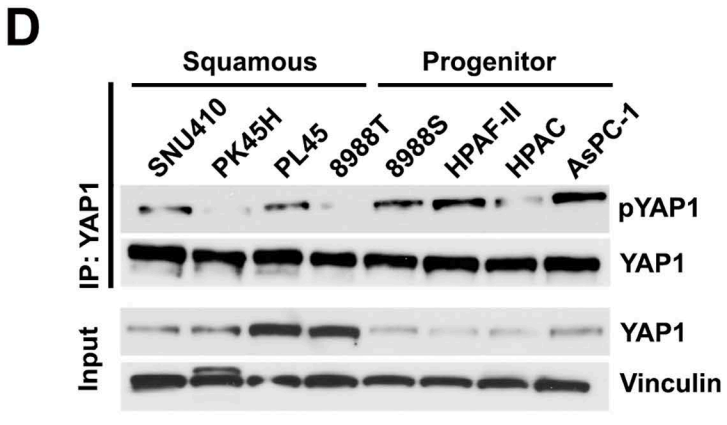

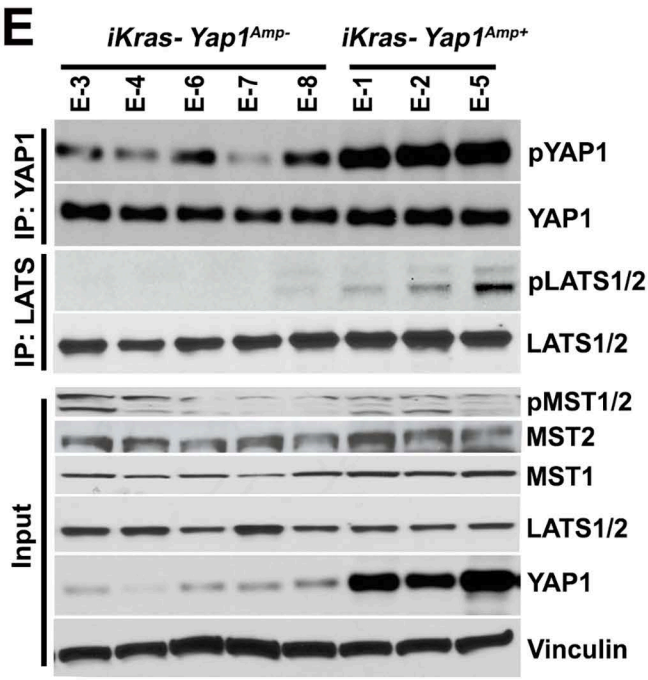

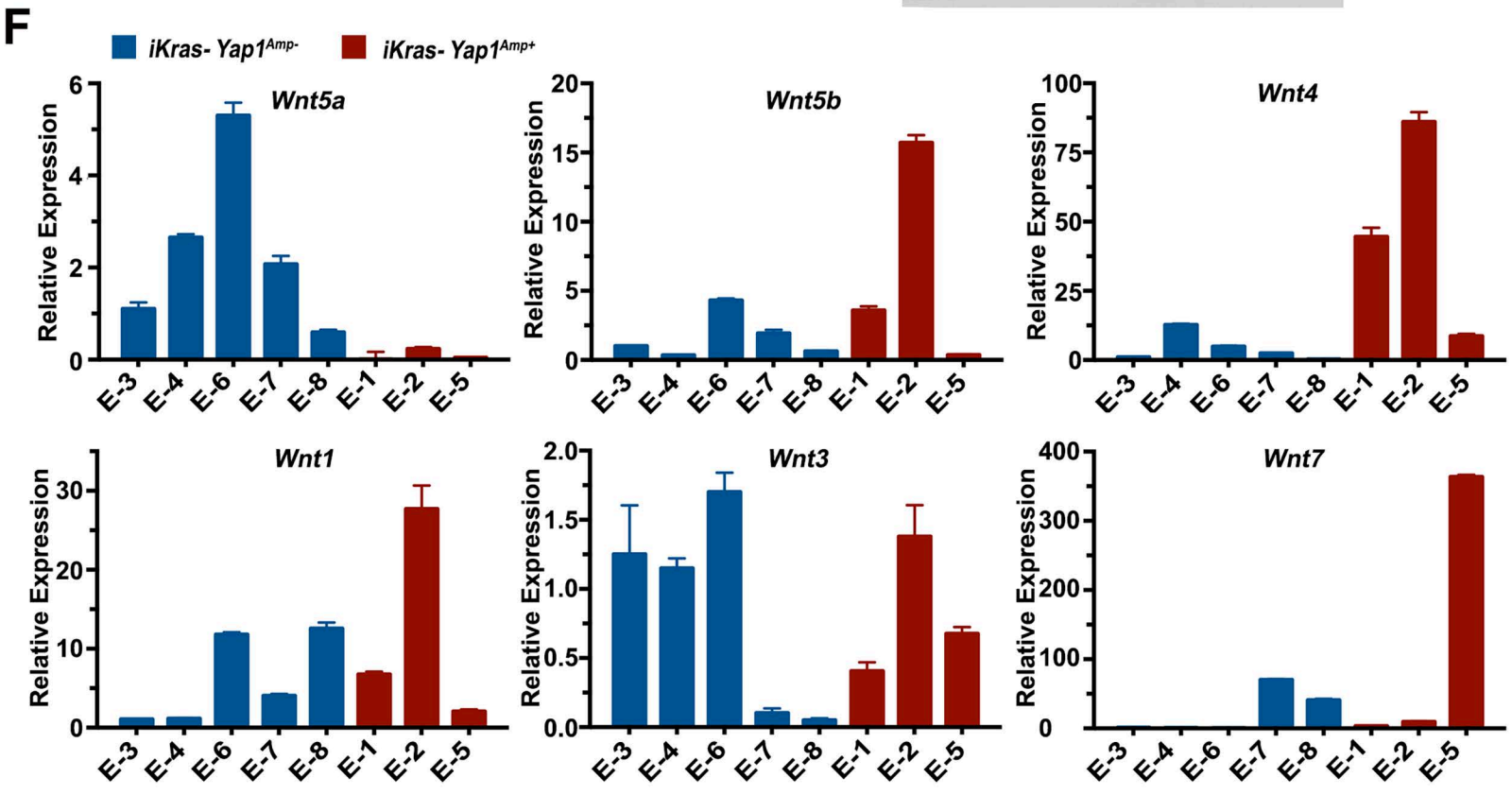

Fig.S4

bioRxiv preprint doi: https://doi.org/10.1101/270314; this version posted February 23, 2018. The copyright holder for this preprint (which was not certified by peer review) is the author/funder. All rights reserved. No reuse allowed without permission.

Supplementary Table 1. YAP1-regulated genes are enirched in signatures for tumor development and metastasis.

NAME	SIZE	ES	NES	NOM p-val	FDR q-val
SHEDDEN_LUNG_CANCER_POOR_SURVIVAL_A6	60	0.50	4.45	0.00000	0.00000
VECCHI_GASTRIC_CANCER_EARLY_UP	61	0.46	4.24	0.00000	0.00000
ROSTY_CERVICAL_CANCER_PROLIFERATION_CLUSTER	41	0.53	4.09	0.00000	0.00000
SARRIO_EPITHELIAL_MESENCHYMAL_TRANSITION_UP	40	0.52	3.94	0.00000	0.00000
RODRIGUES_THYROID_CARCINOMA_POORLY_DIFFERENTIATED_UP	59	0.44	3.92	0.00000	0.00000
WHITEFORD_PEDIATRIC_CANCER_MARKERS	24	0.54	3.18	0.00000	0.00000
ZHANG_BREAST_CANCER_PROGENITORS_UP	31	0.48	3.12	0.00000	0.00000
SENGUPTA_NASOPHARYNGEAL_CARCINOMA_UP	33	0.44	2.98	0.00000	0.00002
WINNEPENNINCKX_MELANOMA_METASTASIS_UP	21	0.53	2.93	0.00000	0.00000
GRADE_COLON_CANCER_UP	60	0.32	2.84	0.00000	0.00002
BIDUS_METASTASIS_UP	20	0.51	2.79	0.00000	0.00006
TURASHVILI_BREAST_DUCTAL_CARCINOMA_VS_LOBULAR_NORMAL_DN	10	0.71	2.77	0.00000	0.00006
WU_CELL_MIGRATION	36	0.39	2.77	0.00000	0.00006
RHODES_UNDIFFERENTIATED_CANCER	12	0.65	2.72	0.00000	0.00008
ZHENG_GLIOBLASTOMA_PLASTICITY_UP	42	0.35	2.71	0.00000	0.00008
GRADE_COLON_AND_RECTAL_CANCER_UP	27	0.44	2.68	0.00000	0.00017
CHIANG_LIVER_CANCER_SUBCLASS_PROLIFERATION_UP	28	0.42	2.63	0.00000	0.00029
SCHUETZ_BREAST_CANCER_DUCTAL_INVASIVE_UP	44	0.34	2.62	0.00000	0.00036
PATIL_LIVER_CANCER	77	0.25	2.45	0.00000	0.00127
HALLMARK_EPITHELIAL_MESENCHYMAL_TRANSITION	36	0.347	2.44	0.00000	0.00109
ACEVEDO_LIVER_TUMOR_VS_NORMAL_ADJACENT_TISSUE_UP	59	0.26	2.33	0.00000	0.00274
LIEN_BREAST_CARCINOMA_METAPLASTIC_VS_DUCTAL_UP	12	0.55	2.33	0.00000	0.00279
PROVENZANI_METASTASIS_UP	17	0.46	2.28	0.00213	0.00375
WOO_LIVER_CANCER_RECURRENCE_UP	16	0.45	2.16	0.00000	0.00695
WANG_ESOPHAGUS_CANCER_VS_NORMAL_UP	17	0.44	2.22	0.00000	0.00485
HUMMERICH_SKIN_CANCER_PROGRESSION_UP	14	0.49	2.21	0.00000	0.00523
RAMALHO_STEMNESS_UP	12	0.50	2.12	0.00000	0.00843
RICKMAN_TUMOR_DIFFERENTIATED_WELL_VS_MODERATELY_DN	10	0.54	2.03	0.00195	0.01402
BORCZUK_MALIGNANT_MESOTHELIOMA_UP	22	0.36	2.01	0.00593	0.01498
OSMAN_BLADDER_CANCER_UP	21	0.35	1.97	0.00380	0.01835
PECE_MAMMARY_STEM_CELL_UP	12	0.47	1.94	0.00777	0.02192
JAEGER_METASTASIS_UP	13	0.45	1.93	0.00195	0.02232
DELYS_THYROID_CANCER_UP	51	0.23	1.89	0.00616	0.02703
ALONSO_METASTASIS_UP	12	0.40	1.69	0.03143	0.06335
VECCHI_GASTRIC_CANCER_ADVANCED_VS_EARLY_UP	20	0.30	1.60	0.04952	0.09008
LIAO_METASTASIS	48	0.19	1.59	0.03106	0.09390

bioRxiv preprint doi: https://doi.org/10.1101/270314; this version posted February 23, 2018. The copyright holder for this preprint (which was not certified by peer review) is the author/funder. All rights reserved. No reuse allowed without permission.

Supplementary Table 2. YAP1-regulated genes are enriched in signatures related to cell proliferation and cell cycle progression, part of GP2 and GP4 gene programs associated with squamous subtype of PDAC* (Bailey et al).

NAME	SIZE	ES	NES	NOM p-val	FDR q-val
CHANG_CYCLING_GENES	39.00	0.54	4.03	0.00000	0.00000
REACTOME_CELL_CYCLE	48.00	0.47	3.88	0.00000	0.00000
REACTOME_CELL_CYCLE	48.00	0.47	3.79	0.00000	0.00000
BENPORATH_CYCLING_GENES	82.00	0.36	3.71	0.00000	0.00000
GO_CELL_CYCLE_PROCESS	91.00	0.34	3.70	0.00000	0.00000
REACTOME_CELL_CYCLE_MITOTIC	40.00	0.50	3.69	0.00000	0.00000
GO_CELL_CYCLE	108.00	0.31	3.60	0.00000	0.00000
HALLMARK_G2M_CHECKPOINT	27.00	0.57	3.55	0.00000	0.00000
REACTOME_DNA_REPLICATION	28.00	0.53	3.39	0.00000	0.00000
GO_REGULATION_OF_CELL_CYCLE	86.00	0.32	3.30	0.00000	0.00000
GO_MITOTIC_CELL_CYCLE	68.00	0.34	3.23	0.00000	0.00000
GO_DNA_REPLICATION	30.00	0.49	3.13	0.00000	0.00000
GO_CELL_CYCLE_PHASE_TRANSITION	31.00	0.49	3.12	0.00000	0.00000
GO_REGULATION_OF_CELL_CYCLE_PROCESS	48.00	0.37	3.02	0.00000	0.00014
REACTOME_MITOTIC_M_M_G1_PHASES	22.00	0.52	2.93	0.00000	0.00000
GO_CELL_DIVISION	39.00	0.40	2.90	0.00000	0.00022
GO_CELL_PROLIFERATION	61.00	0.32	2.85	0.00000	0.00019
REACTOME_G1_S_TRANSITION	16.00	0.59	2.80	0.00000	0.00006
REACTOME_MITOTIC_G1_G1_S_PHASES	19.00	0.54	2.78	0.00000	0.00006
REACTOME_S_PHASE	16.00	0.58	2.78	0.00000	0.00006
GO_CELL_CYCLE_G1_S_PHASE_TRANSITION	17.00	0.59	2.77	0.00000	0.00039
GO_REGULATION_OF_CELL_DIVISION	23.00	0.47	2.70	0.00000	0.00113
GO_REGULATION_OF_MITOTIC_CELL_CYCLE	46.00	0.34	2.68	0.00000	0.00116
REACTOME_SYNTHESIS_OF_DNA	14.00	0.58	2.55	0.00000	0.00062
BENPORATH_PROLIFERATION	22.00	0.46	2.54	0.00000	0.00062
GO_POSITIVE_REGULATION_OF_CELL_PROLIFERATION	66.00	0.28	2.52	0.00000	0.00309
KAUFFMANN_DNA_REPLICATION_GENES	21.00	0.45	2.49	0.00000	0.00098
WHITFIELD_CELL_CYCLE_S	24.00	0.42	2.44	0.00000	0.00135
REACTOME_CELL_CYCLE_CHECKPOINTS	13.00	0.57	2.43	0.00000	0.00137
GO_REGULATION_OF_CELL_PROLIFERATION	127.00	0.19	2.39	0.00000	0.00664
WHITFIELD_CELL_CYCLE_G1_S	22.00	0.40	2.25	0.00419	0.00447
KEGG_DNA_REPLICATION	10.00	0.58	2.24	0.00000	0.00470
REACTOME_M_G1_TRANSITION	10.00	0.58	2.21	0.00606	0.00545
WHITFIELD_CELL_CYCLE_G2_M	23.00	0.38	2.19	0.00000	0.00589
GO_REGULATION_OF_CELL_CYCLE_PHASE_TRANSITION	32.00	0.32	2.12	0.00200	0.01940
WHITFIELD_CELL_CYCLE_G2	29.00	0.32	2.07	0.00000	0.01143
GO_CELL_CYCLE_G2_M_PHASE_TRANSITION	14.00	0.42	1.90	0.01136	0.04134
HALLMARK_MITOTIC_SPINDLE	14.00	0.46	2.04	0.00189	0.01553
KEGG_CELL_CYCLE	16.00	0.40	1.87	0.01202	0.02866
FIRESTEIN_PROLIFERATION	13.00	0.38	1.64	0.03725	0.07637

*Mitotic G2-G2/M phases(R): GP4 (p=0, FDR<3.846e-05); GP2 (p=0.0097, FDR=0.06118).

*Mitotic Spindle: GP4 (P=0.0002, FDR=0.002811)

bioRxiv preprint doi: https://doi.org/10.1101/270314; this version posted February 23, 2018. The copyright holder for this preprint (which was not certified by peer review) is the author/funder. All rights reserved. No reuse allowed without permission.

Supplementary Table 3. YAP1 targets are enriched in gene signatures associated with well known oncogenic signaling pathways and gene programs associated with squamous subtype of PDAC* (Bailey et al).

Validated targets of C-MYC transcriptional activation(N)*

NAME	SIZE	ES	NES	NOM p-val	FDR q-val
HALLMARK_TNFA_SIGNALING_VIA_NFKB	42	0.42	3.16	0.00000	0.00000
HALLMARK_MYC_TARGETS_V2	10	0.67	2.57	0.00000	0.00000
HALLMARK_MYC_TARGETS_V1	12	0.57	2.41	0.00000	0.00091
MYC_UP.V1_UP	14	0.45	2.06	0.00000	0.01826
DANG_BOUND_BY_MYC	71	0.28	2.69	0.00000	0.00017
DANG_MYC_TARGETS_UP	10	0.61	2.37	0.00000	0.00220
BILD_MYC_ONCOGENIC_SIGNATURE	23	0.39	2.30	0.00411	0.00350
ALFANO_MYC_TARGETS	24	0.32	1.82	0.01613	0.03544

*GP5 (P=0, FDR<1.000e-04), GP4 (P=0.0021,FDR=0.01989), GP2 (P=0.016, FDR=0.08453)

IL6-mediated signaling events(N)*

NAME	SIZE	ES	NES	NOM p-val	FDR q-val
CROONQUIST_IL6_DEPRIVATION_DN	23	0.64	3.60	0.00000	0.00000
DAUER_STAT3_TARGETS_UP	11	0.50	2.07	0.00382	0.01121
HALLMARK_IL6_JAK_STAT3_SIGNALING	11	0.39	1.62	0.04211	0.07865

*GP2 (P=0.0157, FDR=0.0835)

E2F transcription factor network(N)*

NAME	SIZE	ES	NES	NOM p-val	FDR q-val
HALLMARK_E2F_TARGETS	39	0.54	3.93	0.00000	0.00000
E2F1_UP.V1_UP	21	0.54	2.94	0.00000	0.00075
ISHIDA_E2F_TARGETS	13	0.58	2.56	0.00000	0.00058
PID_E2F_PATHWAY	14	0.51	2.33	0.00199	0.00275
BILD_E2F3_ONCOGENIC_SIGNATURE	32	0.31	2.08	0.00000	0.01104

*GP4 (P=0; FDR<4.762e-05)

RhoA signaling pathway(N)*

NAME	SIZE	ES	NES	NOM p-val	FDR q-val
BERENJENO_TRANSFORMED_BY_RHOA_UP	82	0.47	4.81	0.00000	0.00000

*GP3 (P=0.0029, FDR=0.02324)

TGFB/BMP Receptor Signaling*

NAME	SIZE	ES	NES	NOM p-val	FDR q-val
LEE_BMP2_TARGETS_DN	90	0.49	5.27	0.00000	0.00000
TGFB_UP.V1_UP	23	0.42	2.39	0.00000	0.00526
COULOUARN_TEMPORAL_TGFB1_SIGNATURE_UP	13	0.53	2.29	0.00000	0.00361
KARLSSON_TGFB1_TARGETS_UP	10	0.58	2.19	0.00199	0.00587
PLASARI_TGFB1_TARGETS_10HR_UP	36	0.29	1.93	0.00853	0.02192
MCBRYAN_PUBERTAL_TGFB1_TARGETS_UP	19	0.33	1.69	0.02863	0.06292

*BMP receptor signaling(N):GP3 (P=0.0001, FDR=0.001106)

bioRxiv preprint doi: https://doi.org/10.1101/270314; this version posted February 23, 2018. The copyright holder for this preprint (which was not certified by peer review) is the author/funder. All rights reserved. No reuse allowed without permission.

TNF signaling pathway(K)*

NAME	SIZE	ES	NES	NOM p-val	FDR q-val
HALLMARK_TNFA_SIGNALING_VIA_NFKB	42	0.42	3.16	0.00000	0.00000
PHONG_TNF_TARGETS_UP	15	0.65	2.99	0.00000	0.00000

*GP2 (P= 0.0004; FDR=0.008161)

bioRxiv preprint doi: https://doi.org/10.1101/270314; this version posted February 23, 2018. The copyright holder for this preprint (which was not certified by peer review) is the author/funder. All rights reserved. No reuse allowed without permission.

Supplementary Table 4. Yap1 targets in this study are enriched in Hippo signaling pathway (GP3) of squamous subtype (Bailey et al)

Bailey et al.	This study
Hippo signaling pathway(K) GP3_Reactome (p=0, FDR<7.692e-05)	**Pa04C-YAP^{S127A} (Fold Change)**
FZD10	128.00
WTIP	20.22
FGF10	12.90
TCF7L1	10.00
TGFB1	9.70
BMP8A	7.06
TGFBR1	6.80
BMP6	5.81
SMAD7	5.57
CTGF	3.28
TGFB3	2.80
LATS2	2.17
SNAI2	2.05
TEAD1	1.71
GLI2	0.49
FZD2	0.43
LEF1	0.10
DLG4	0.08